İSTANBUL TECHNICAL UNIVERSITY ★ INSTITUTE OF SCIENCE AND TECHNOLOGY

EFFECTS OF ANISOTROPY ON FORMABILITY IN SHEET METAL FORMING

M.Sc.Thesis by
Göktuğ ÇINAR, B.Sc.

Department: Mechanical Engineering
Programme: Solid Mechanics

JUNE 2006

İSTANBUL TECHNICAL UNIVERSITY ★ INSTITUTE OF SCIENCE AND TECHNOLOGY

EFFECTS OF ANISOTROPY ON FORMABILITY IN SHEET METAL FORMING

M.Sc.Thesis by
Göktuğ ÇINAR, B.Sc.
(503021510)

Date of submission : 24 April 2006
Date of defence examination: 16 June 2006

Supervisor (Chairman): Assoc. Prof. Dr. Erol ŞENOCAK

Members of the Examining Committee: Prof. Dr. Mehmet DEMİRKOL

Prof. Dr. Süleyman TOLUN

ACKNOWLEDGMENTS

I would like to thank my supervisor Assoc. Prof. Dr. Erol Şenocak for his constructive comments and patience throughout the course of this thesis.

Sincere appreciations go to my parents for their continuous encouragements and never ended supports.

April 2006 Göktuğ ÇINAR

TABLE OF CONTENTS

ABBREVIATIONS

BHF : Blankholder Force
CAD : Computer Aided Design
FEM : Finite Element Method
FEA : Finite Element Analysis
FLC : Forming Limit Curve
FLD : Forming Limit Diagram
FCC : Face Centered Cubic
BCC : Body Centered Cubic

LIST OF TABLES

LIST OF FIGURES

Page No

LIST OF SYMBOLS

E	: Young's modulus
F , H, G, N	: Hill48 yielding criteria coefficients
K	: Material strength coefficient
m	: Strain rate exponent
n	: Strain hardening exponent
r	: Plastic strain ratio
R	: Normal anisotropy coefficient
r0	: Lankford coefficient with respect to rolling direction 0
r45	: Lankford coefficient with respect to rolling direction 45
r90	: Lankford coefficient with respect to rolling direction 90
Δr	: Earing tendency coefficient
t	: Sheet thickness
e	: Engineering strain
ε	: True strain
ε_w	: Width strain
ε_t	: Thickness strain
u	: Displacement of the material
v	: Velocity of the material flow
v_x, v_y, v_z	: Flow component in the x direction
t	: Measure of time
$\dot{\varepsilon}_x, \dot{\varepsilon}_y, \dot{\varepsilon}_z$	: Strain rate components
$\dot{\gamma}_{xy}, \dot{\gamma}_{yz}, \dot{\gamma}_{xz}$	: Shear strain rate components
σ_y	: Yield stress
$\bar{\sigma}$	: Effective Stress
$\bar{\varepsilon}$	: Effective Strain
w	: Sheet width
μ	: Coefficient of friction

SAC METAL ŞEKİLENDİRMEDE ANİSOTROPİNİN ŞEKİLLEDİRİLEBİLME ÜZERİNDEKİ ETKİSİ

ÖZET

Sac şekillendirme simulayonlarının önemi son yıllarda otomotiv endüstrisinin gelişmesine bağlı olarak artmıştır. Üreticiler, zorlaşan piyasa koşullarında rekabetçi güçlerini koruyabilmek amacıyla maliyetleri düşürmek durumundadırlar. Bu amacla işletmeler sonlu elemanlar yöntemlerini, kalıp üretim aşamasından başlayarak deneme sayılarının azaltılması, malzeme kontrolleri, ekipman dayanım kontrolleri gibi uygulamalarda kullanmaktadır.

Otomobil panellerinin üretiminde kırışma, yırtılma, aşırı incelme, yüzey bozulması ve geri yaylanma gibi kusurlar oluşur. Bu kusurların giderilmesi amacıyla, kalıp yüzeylerinin geometrisi, sac malzemenin yapılacak işlemler için uygunluğu, sac malzemenin kalıp boşluguna akışı, pot çemberi kuvvetinin ayarlanması, kalıp ve sac malzeme arasındaki sürtünmenin etkisi, süzdürme çubuklarının konumları ve geometrisi gibi durumlar imalat öncesinde simülasyon programları ile tesbit edilir.

Bu çalışmada, ticari simülasyon programları kullanılarak bir otomobil tekerlek yuvası panelinin kalıp yüzeylerinin elde edilmesine dolayısıyla kullanılacak panelin elde edilmesine çalışılmıştır. Çalışmanın ikinci bölümünde bu panelin prosesinde önemli olan işlemler ve literatürde gecen bazı genel kavramlar açıklanmıştır. Üçüncü bölümde sac şekillendirmeye etki eden faktörler ve ortaya çıkabilen kusurlar anlatılmış, bazı durumlar işparçamızla örneklendirilmiştir. Dördüncü bölümde matematiksel malzeme yüzey akış bünye denklemleri, izotropi, anizotsopi kavramları ve ilgili temel ifadeler anlatılmıştır. Beşinci bölümde ise, panelin değişik durumlardaki karşılaştırmalı çekme simülasyonları yer almaktadır. Son bölümde ise bu çalışmadan çıkarılabilen sonuçlar ve gelecekte yapılabilecek benzer bir çalışma için düşünülebilecekler anlatılmıştır.

EFFECTS OF ANISOTROPY ON FORMABILITY IN SHEET METAL FORMING

SUMMARY

In recent years, significance of sheet forming simulations have risen with respect to development of automobile industry. Manufacturers, have to reduce the costs to remain competitive in the compelling market conditions. For this reason, finite element simulations are used for the die making stage to reduce number of try-outs, to make better material selections and controls for endurance limits of the tools.

During the manufacturing of automobile panels, failures such as wrinkling, tearing, thinning, surface distortion and springback can be observed. Geometry of die surfaces, material selection, friction between blank and die, blankholder force locations and geometry of the drawbeads are searched with simulation softwares.

In this study, commercial simulation software is used to figure out the parameters of the dies for the automobile wheelhouse panel. In the second chapter, literature survey was made for the process of this panel and some general concepts. In the third chapter, the factors and failures that affect formability were observed . In the fourth chapter, information about isotropy, anisotropy, constitution laws and yielding equations were examined. Results of the analyses of the wheelhouse panel are shown in the fifth chapter. Conclusions and recommendations were made in the last chapter.

1.INTRODUCTION

Sheet metal forming operations are the common methods for shaping sheet metals plastically between tools (dies), into desired final configuration. Thus, simple part geometry is transformed into a complex one, whereby the tools "store" the desired geometry and impart pressure on the deforming material through tool/material interface **[15]**.

A sheet metal forming system is composed of all the input variables such as the blank (geometry and material), the tooling (geometry and material), the conditions at the tool/material interface, the mechanics of plastic deformation, the equipment used, the characteristic of the final product and finally the plant environment where the process is being conducted. The application of the system approach to sheet metal forming is illustrated in Figure 1.1, as applied to deep drawing. The "systems approach" in sheet metal forming allow the study of the input/output relationships and the effects of process variables on product quality and process economics. To obtain the desired shape and properties in the product, the metal flow should be well understood and controlled. The direction of flow, the magnitude of deformation, and the temperature involved greatly influence the properties of formed products. **[15]**

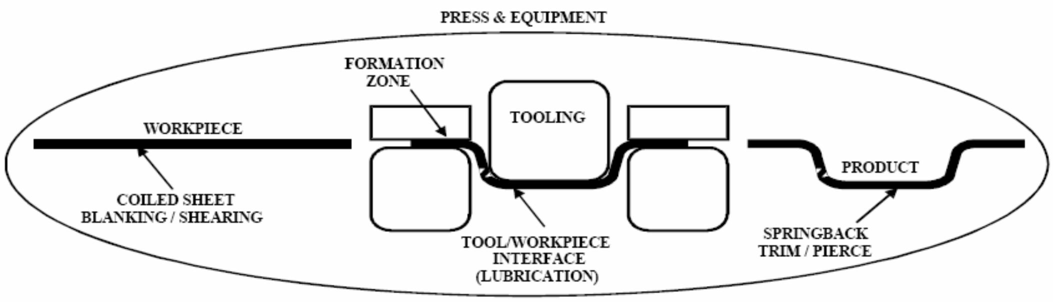

Figure 1.1: Schematic of system approaches (Deep Drawing)

2.LITARATURE SURVEY

2.1 Introduction

In a literature search, one can find many kinds related with sheet metal operations. In this thesis, a process of wheelhouse panel is examined. In this point of view, applied operations to obtain the final shape of wheelhouse panel will be taken into consideration to narrow the literature survey.

2.2 Deep Drawing

For sheet metal forming simulation the most relevant process is deep drawing, which will be described in the following.

Deep drawing is a sheet metal forming process where a (plane) sheet of metal is given a double curved shape through drawing, compression and flattening.Examples of products manufactured with this process are different vessels, body panels for cars, airplane components, etc. The sheet of metal is placed between the two halves of the tooling, the die and the binder. The purpose of the die and the binder is to hold the sheet with enough force (the binder force) to avoid that wrinkles occur. When the punch is moved down against the surface of the sheet it pushes the sheet down in to the die and the sheet will start to bend **[2, 5]**.

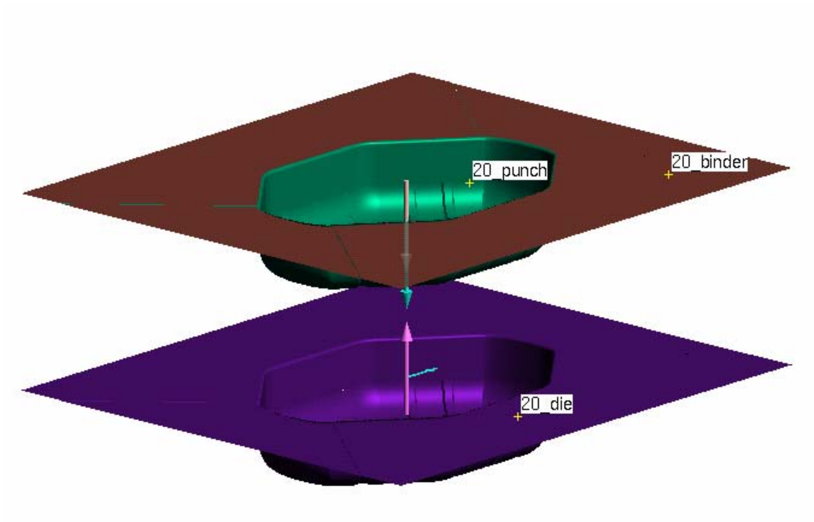

Figure 2.1: Schematic of the deep drawing process

Figure 2.2: Panel geometry after deep drawing operation

A deep drawn wheelhouse panel is seen in figure 2.2. The panel is ready for the following operations such as trimming, flanging and restrike.

As a mostly used process, deep drawing can be explained in four time steps.

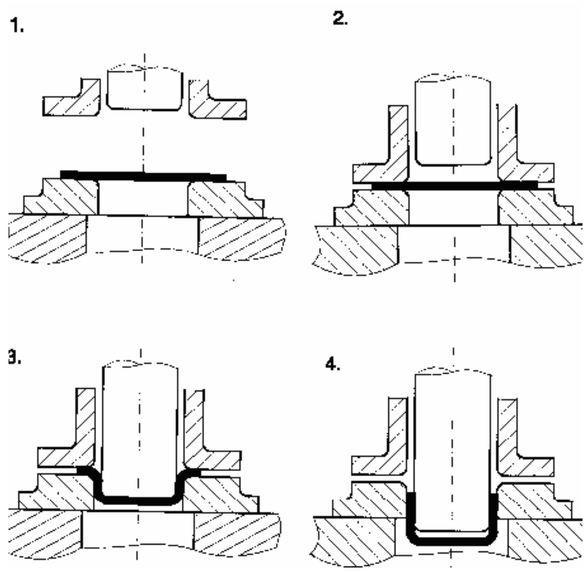

Figure 2.3: The deep drawing process in four time steps [2]

The four steps illustrated are as follows:

1. A cut through the tool set up shows the punch, die and metal sheet (or workpiece) on the binder. The binder is in an uplifted position.

2. The binder and punch is moved downwards. The binder reaches the sheet ahead of the punch and thereby a pressure, the binder force, is applied on the sheet. Hence the peripheral parts of the workpiece are kept in place. If the binder is not flat an initial forming takes place.

3. The punch is now in contact with the sheet and the sheet is drawn through the opening in the die. It slides over the die radius. As the punch proceeds downwards the outer radius of the circular workpiece is reduced. In this process the workpiece is formed through stretching in the drawing direction, accompanied by compression and flattening in the circular direction.

4. The punch moves back upwards and the formed component is pushed out of the tool **[2]**.

2.3 Flanging

Flanging is a forming operation in which a narrow strip at the edge of a sheet is bent along a straight or curved line. Compared to plane strain bending, flanging is applied on the edges of parts, and the flange length is relatively small. As shown in figure 2.4, a typical bend angle in flanging is 90^{o} **[5, 17]**.

During manufacturing, the sheet metal goes through different dies on its way to a finished product. After deep drawing, the excess metal is usually trimmed off, and flanged. Flanging is often a strengthening requirement in the design or to provide a mating surface for subsequent joining operations. During stretch flanging, a tensile strain is usually imposed on the sheared edge, causing splitting failure in some cases. Determination of the sheared edge forming limits is usually conducted by stretching a punched hole, thereby evaluating formability of the sheared edge **[5, 22]**.

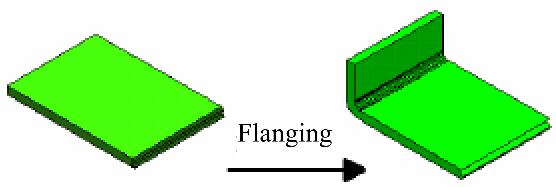

Figure 2.4: Schematic of flanging operation

A typical flange tooling is shown in the figure 2.5 below, this tooling includes a die, pad and a punch. The die should be sufficiently hard to maintain the proper flange radius, but should also be tough enough to resist corner chipping. The pad applies pressure to the sheet metal to clamp the part and avoid the part lifting during the flanging process. The punch forming the outside flange surface may be highly stressed. Therefore, it is made of hardened tool steel **[17]**.

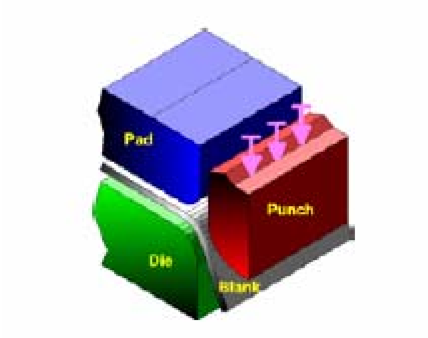

Figure 2.5: Flange Tooling

Due to type of the mating of the surfaces related to the flanges, type of flanges might be varied. By using different geometric dies, one can obtain flanges as shown in figure 2.6 below.

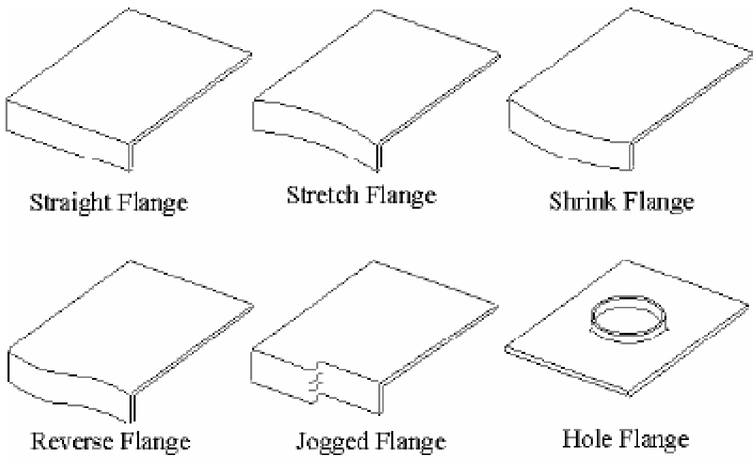

Figure 2.6: Types of flanging [32]

Figure 2.7: Flanging operation of the wheelhouse panel

It is important to mention about the failures during the flanging operation.Figure 2.8 shows the major defects of bending and flanging, which are fracture, indenting folding, necking, wrinkling and calling.

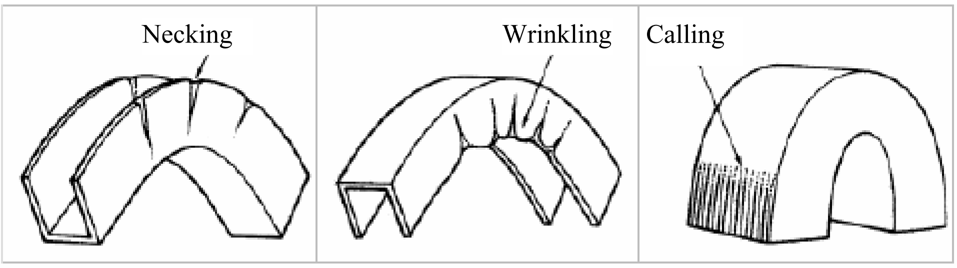

Figure 2.8: Failures occur during flanging operations

The following chart, **Figure 2. 9**, lists the major flanging variables:

• Die Radius

• Punch Radius

• Clearance Ratio

• Pad Force

And their effects on flanging process:

• Springback

• Die load

• Recoil / Warp

• Minimum Bend Radius (or maximum curvature)

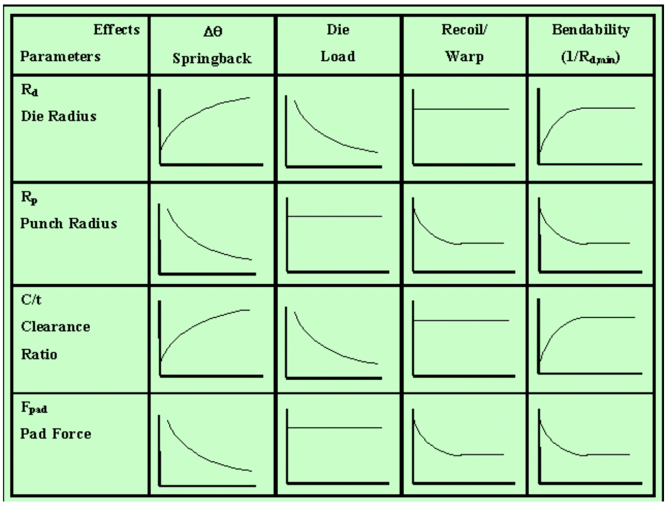

Figure 2.9: Graphs of the effects of different variables on flanging

2.4 Trimming

During any press working operation in which the part must be held in place by the press, the outer edge of the part, which is the area usually gripped, becomes marked and scored. Trimming is the cutting off of the excess metal edge. This operation might be the last to be performed in a progressive die in order to separate the parts from the strip. Trimming may be performed vertically or horizontally, depending on the part configuration [5, 20].

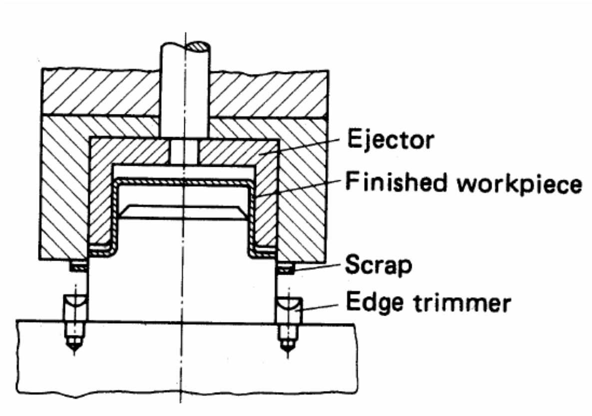

Figure 2.10: Trimming process [20]

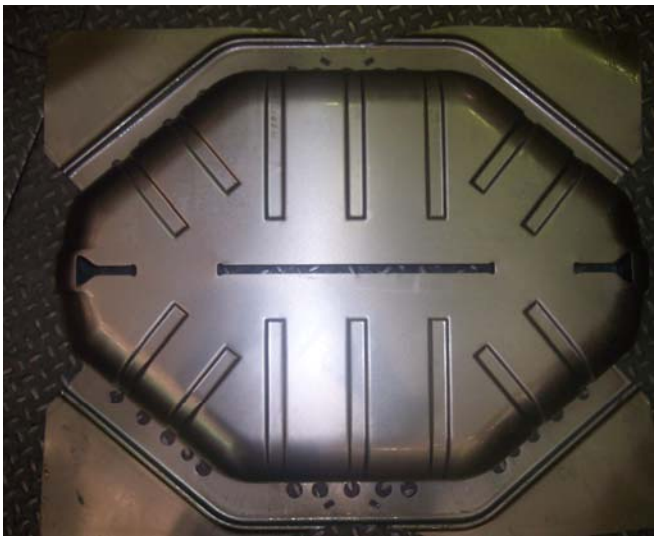

Figure 2.11: Panel geometry before trimming process

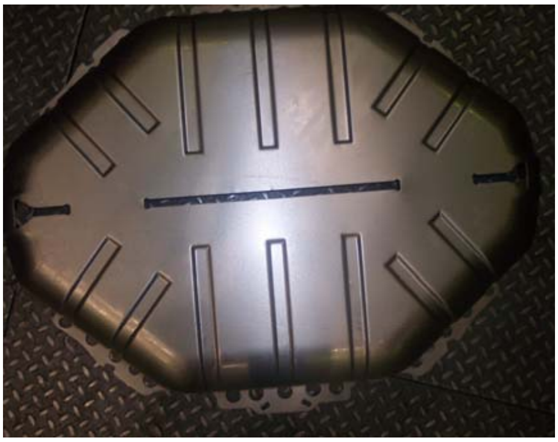

Figure 2.12: Panel geometry after trimming process

2.5 Restrike

When the tools are removed away after the operation, internal forces caused the elastic recovery. This recovery can be observed in the bending, bending-unbending, reverse bending areas. This is one of the major problems in die making field because of the aligning and mating problems during the assembly process of the panels.

This phenomenon is called sprinback and it has to be compansated by overcrowning and overbending techniques on the die surface. Another technique for the compansation is the restrike operation. The restrike die hits the areas where compansation is needed and prepares the panel for the following operations.

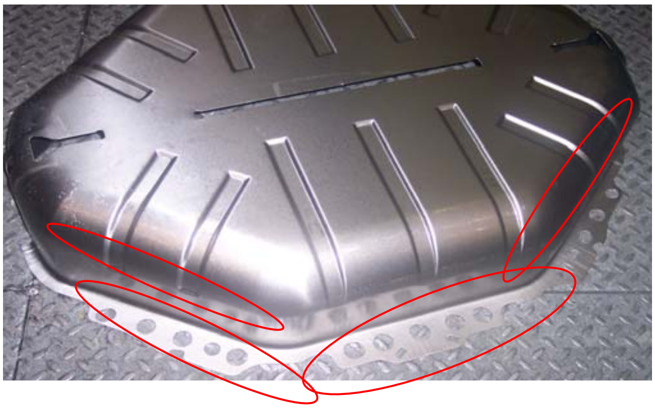

Figure 2.13 : Areas that are restriked

3. FORMABILITY OF SHEET METALS

3.1 Introduction

The industrial metal working process of sheet metal forming is strongly dependent on numerous interactive variables: material behaviour, lubrication, forming equipment etc. One of the main limitations in industrial stampings seems to be the appearance of localized necking. The mathematical ability to deform plastically depends on a great number of interactive parameters whose experimental study is a difficult task. The theoretical analysis of the plastic instability is therefore of major importance in order to predict the forming limit strains, examine the influence of each parameter on the necking occurrence and improve press performance. From this view, forming limit diagram represents a useful concept on sheet metal formability characterization and very important safety tool in sheet metal forming simulation which is written in the next section [14, 27].

The quality of a stamped commercial part is largely influenced by the material flow within the tools during the sheet metal forming operation. Therefore it is important to control the material flow rate to avoid defects such as wrinkling, tearing, surface distortion and springback. Furthermore, in car body manufacturing it is important that outer panels should be subjected to sufficient straining because of the flex resistance (or dent resistance) [19, 24]. Often, it is desirable to increase material flow by using lubricants to reduce stress. In other situations, it is common practice to reduce flow by introducing additional restraining force.

Generally, the material flow is controlled by the blankholder: a restraining force is created by friction between the tools and the blank. As a result, the tensile stresses are increased, material flow is controlled, and the formation of wrinkles is avoided.

3.2 Blank Holder

Blank holder force plays a major factor in the formability of sheet metals. If the blank holder force is too low, then wrinkling in the flange or the wall will occur. If the blank holder force is too high, then excessive thinning or fracture occurs. A typical drawability chart is shown in Figure 3.1. In this chart, the blank holder force is shown along the x-axis and the draw depth is along the y-axis. The two lines on the chart shows the limits of wrinkling and fracture. During the design phase, a blank holder force must be selected with a large enough drawability window to account for variances in tooling and press setups.

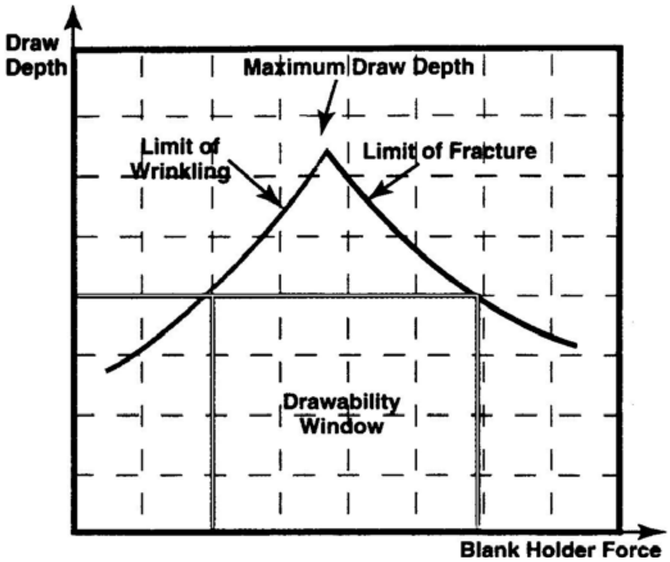

Figure 3.1: Drawability chart [18].

Formability can be increased by varying blank holder force throughout the press stroke. Blank holder force can be increased, decreased, or kept constant as a function of press stroke depending on the particular forming operation. If fracture occurs later in the stroke, then blank holder force should decrease with press stroke. If wrinkling occurs later in the stroke, then blank holder force should increase with press stroke. Typically, the BHF is reduced to account for the reduction of drawing ratio that occurs through the stroke. Each part needs to be considered separately in order to develop a proper blank holder force application scheme [19].

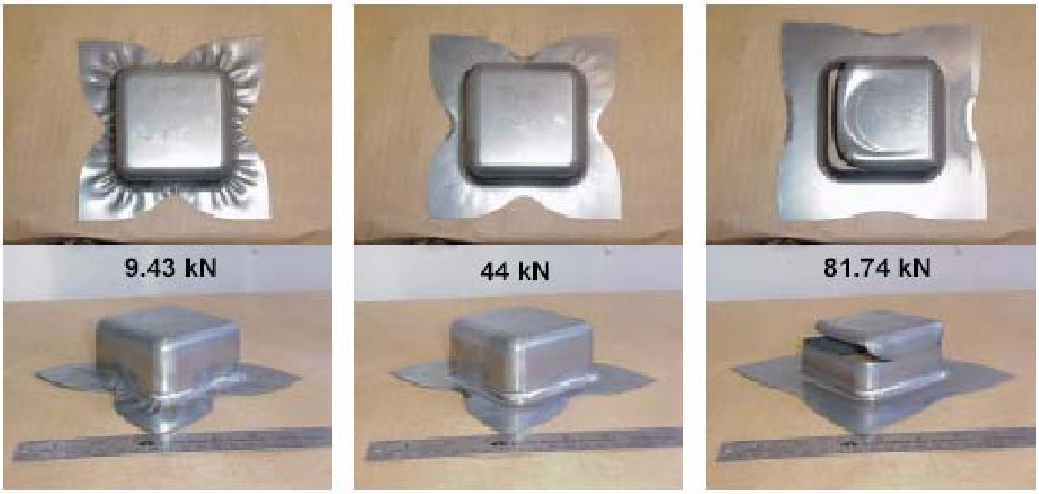

Figure 3.2: Effect of blankholder force on formability of the material [11].

However, during the forming stage, the blankholder does not make contact with the entire blank which means that it cannot fully control the material flow [11]. Moreover, when a higher restraining force is needed, higher blankholder force must be applied. To reduce the flow of material between the binder faces or increase restraining force, it is not good practice to simply keep increasing the blankholder force. This results in higher stress values being imposed on the die and press which may cause excessive wear in the tools and galling in the blank.

3.3 Drawbeads

In some cases the minimum blankholder force required to provide the necessary restraining force for a successful drawing operation may exceed the tonnage capacity of the press. Therefore, a local control mechanism is desired which restrains the material flow sufficiently at relatively low blankholder force. These demands can be fulfilled by drawbeads, which are rib-like projections mounted on either the binder or the draw ring surface that restrict and control metal flow into the die cavity and over the punch of a draw die (see Figure 3.3). Drawbeads are an important characteristic of blankholder control and are used to supplement friction and obtain more uniform deformation [11].

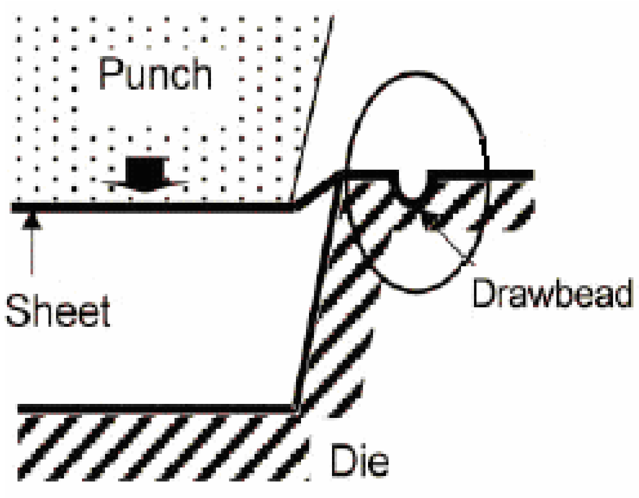

Figure 3.3: Schematic of a stamping process including drawbeads [11].

3.4 Forming Limit Diagram

In all sheet metal forming operations, one has to care about the state of the blank until the final shape is obtained. Using forming limit diagrams are the most convenient way to avoid failures in the operations. The forming limit diagram offers the chance to determine process limitations in sheet metal forming and it is used in the estimation of stamping characteristics of sheet metal materials. The FLD is usually applied in method planning method planning, in tool construction and in tool shops for optimizing stamping tools and their geometries. With the help of the form modification analysis and the comparison with the FLD, an optimisation of the parameters that influence stamping process such as tool geometries, press pad pressure, lubrication, material will result. A further important area for FLD is in the field of numerical simulations of transformation processes. The FLD of the used material is a necessary prerequisite for the estimation of the simulation results [6].

The early work of Keeler and Backofen (1963) showed that a critical combination of major and minor strains would lead to localized necking. The work of both Keeler and Goodwin (1968) led to the construction of a FLC in principal strain space where any combination of strains above the curve presents some probability of failure (i.e. necking or splitting). formability of sheet materials. Some examples of this research

include attempting to identify the optimum method for constructing the FLC, developing a theoretical framework for predicting strain localization and studying the effects of strain path on the FLC. However, the biggest impact of the FLC has been in the press shop **[6,10,28].**

Stamping industry has benefited from this technology to evaluate and improve the quality of automotive stampings. Typically, a grid of small circles is electrochemically etched onto a blank that is then stamped. During the forming process, the circle grid deforms with the sheet material. Principle strains ε_1 and ε_2 can be determined by measuring the length of grids of circles which are change regarding the maximum length in a circle named major strain and minimum length named minor strain. After measurement, values are converted to the logaritmic values to be considered in the forming limit diagram. The major strain is calculated by the change of the circle diameter in primary deformation direction and minor strain is by the change of diameter in secondary deformation direction .

By comparing the dimensions of the deformed circles (i.e. ellipses) with the original circle diameter, it is possible to measure the surface strains in the critical forming areas of the part and compare them to the FLC for that particular material. This reveals the forming severity of the stamping operation, even when necking or splitting cannot be detected **[28].**

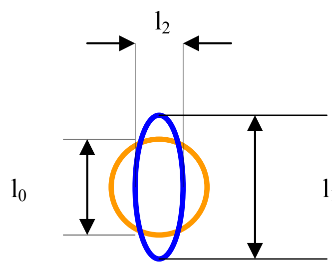

Figure 3.4: Schematic of circle grid deformation

$$\varepsilon_1 = \ln\frac{l_1}{l_0} \qquad \textbf{(3.1)}$$

$$\varepsilon_2 = \ln\frac{l_2}{l_0} \qquad \textbf{(3.2)}$$

By naming ε_1 as major strain and ε_2 as minor strain, one can figure out forming limit curve (FLC) for metarials by experiments which gives the boundaries of the safe region. Failure occurs in the case of exceeding the forming limit curve upwards.

In the Figure 3.5, forming limit curve can be seen. The curve describes the level of strain that the actual material could withstand without failure.

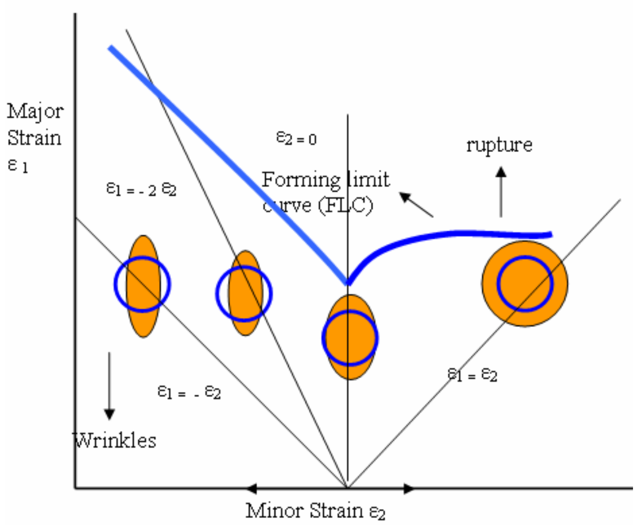

Figure 3.5: State of the strains [2]

Following a rule of thumb experience to assure that the component not will break the strain level should not exceed 80% of the level of the forming limit curve [2].

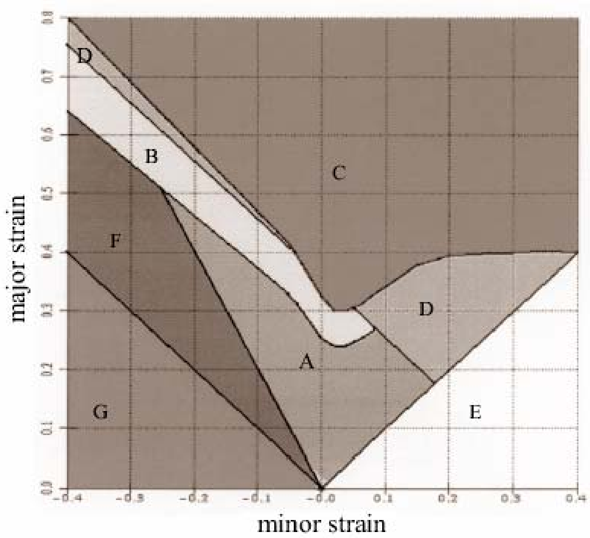

Figure 3.6: Regions of the FLD [2]

Indicated areas in the figure 3.6 help to determine the state of the component after forming operation or operations are made [2].

A. Recommended!. Safe region, appropriate use of the forming abilities of the material

B. Danger of rupture or cracking.

C. The material has cracked.

D. Severe thinning.

E. Insufficient plastic strain, risk of spring back

F. Tendency to wrinkling.

G. Fully developed wrinkles (or thickening).

In general, forming limit diagram inspections made with hand made calculations, but recently, development of image processing technologies and high resolution cameras help to do this analyses by computer programs. However, general concept of inspection does not change.

3.5 Failures in sheet metal forming operations

There are potential formability problems typically associated with each forming operation. The major problems are fracture, buckling and wrinkling, shape distortion, and undesirable surface textures. It is important to recognize and understand which defects are associated with a given process and their effects on the finished workpiece. Not all failures are purely functional (see figure 3.7). Some defects, such as stretcher-strains, may not affect the functionality of the part but may make the part unusable due to aesthetic considerations [14].

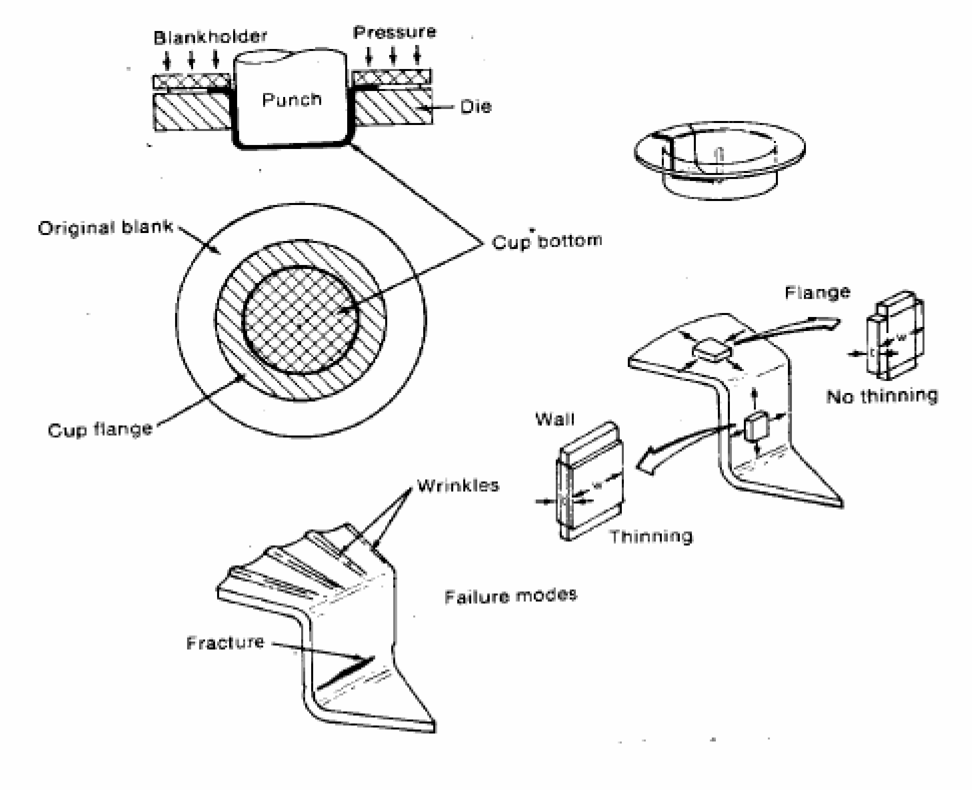

Figure 3.7: Forming defects associated with deep drawing [14].

3.5.1 Fracture

Fracture occurs when a sheet metal blank is subjected to multi axial forces that exceed the failure limits of the material under the given conditions [14].

The common failure of a drawing operation is rupturing of metal in a critical area (see Figure 3.9) because of insufficient strength to withstand the force required to draw the metal from the blank area into the die. The power to cause flange deformation, bending and overcoming friction is supplied by the punch to the deformation region through wall tension. Hence as along as the wall tension remains elastic, no tearing is expected. But if the tensile force exceeds the ultimate tensile strength of the sheet material, then tearing occurs [19].

Various sheet failures and state of the strains are shown in figure 3.8. Understanding this graph will help to prevent these failures with using FLD.

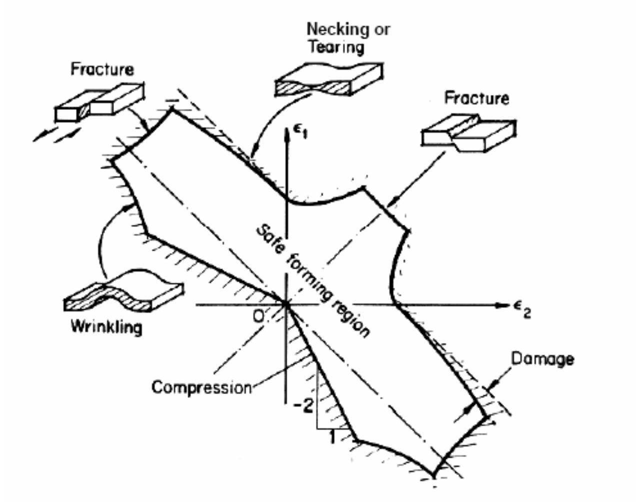

Figure 3.8: Various sheet failures shown on a forming limit diagram

In figure 3.9, the effect of lubrication can be observed. If lubricate is not used, panel fails in the drawing operation.

Figure 3.9: Fractures occured during production

The following factors determine if the cup wall has sufficient strength to avoid tearing [19].

1. The contour of the punch edge and the contour of the die edge
2. The lubrication conditions between the blank and the blank holding surfaces and the die
3. Material properties (K and n)
4. Speed of the press

Tearing might occur due to the following factors:

1. Die radius being too small
2. Die clearance being too small
3. Punch velocity is too high
4. Blank holder pressure is too high

3.5.2 Buckling and wrinkling

In a typical stamping operation, the punch contacts the blank, stretches it, and starts to pull it through the blankholder ring. The edges of the sheet are pulled into the regions with progressively smaller perimeters. This is the reason for the compressive stresses in the circumferential direction. Buckling occurs when these stresses reach a critical level, which is characteristic of the material and its thickness. If the blankholder pressure is not sufficient, buckling may form waves known as wrinkles [14].

When the ratio of tensile stress to compressive stress is large, buckling may take place at lower compressive stress than in the case of unidirectional compression. The effective plastic strain at the buckling point, however, is larger in the case of the sheet which is subjected to biaxial compressive-tensile stress than in the case of the sheet which is subjected to uniaxial compressive stress. In most sheet metal forming processes such as the spherical cup deep drawing process and the cylindrical cup deep drawing process, the deformation path during the forming process and the values of effective plastic strain at the final deformed state are almost the same regardless of the sheet material. It is because the total strain is determined mainly by the geometry of the tool. The comparison of the buckling behavior at the fixed value of effective plastic strain is, therefore, considered to be reasonable. When the ratio of tensile stress to compressive stress is larger than a certain value, buckling does not take place until the fixed value of effective plastic strain is reached. The critical stress ratio above which buckling does not take place can be treated as a convenient measure of the compressive instability tendency of a sheet **[24].**

From a mechanics point of view, the wrinkles are caused by the compression instability, but not all the compression instability conditions result in the wrinkle failures during sheet metal forming. In fact, the wrinkle failures with many cases are mostly depended on the geometry of parts and material properties of blanks. If the geometry of parts and material properties of blanks are matched well, the wrinkle problems can be reduced fully. Now we discuss the wrinkle problems just around a deformation area in sheet plane with one elongation and compression **[3].**

Wrinkling may be a serious obstacle to implementing the forming process and assembling the parts, and may also play a significant role in the wear of the tool. In order to improve the productivity and quality of products, the wrinkling problem must be solved. At present, sheet metal forming processes are widely used in various industrial sectors such as automotive, electric home appliance, and aircraft industries. Also, the needs for high precision and high value-added products are increased. In order to reduce the process development time, the prediction of defects and the modification of design in the design stage are needed **[24].**

3.5.3 Shape Distorsion

It occurs when the residual stresses on the outer surfaces are different from those on the inner surfaces. When these stresses are not compensated by the geometry of the part, relaxation will cause a change in the part shape known as shape distortion **[14].** Residual stresses may also cause geometric distortions in the part. Large-scale distortions may take the form of highs or lows in the part surface or as oil canning (elastic instabilities). Small scale distortions may take the form of rabbit earing, pie crust, crow's feet, or teddy bear ears **[19].**

3.5.4 Orange Peels and Stretcher-Strain Markings

During the stretching of some metals, especially aluminum-magnesium alloys and some low carbon steels, visible localized yielding, called stretcher-strain markings, occur. They are extremely undesirable because of their negative influence on the surface quality of the parts. Painting cannot usually conceal this highly visible phenomenon. Therefore, these sheets cannot be used as outer auto body panels **[14].** Undesirable surface textures such as orange peel or stretcher strain markings may also occur during deformation. Orange peel consists of a rough surface appearance typically caused by the variation of flow stress properties of the various grains contained in the material. Two types of stretcher strains are observed. The first type is caused by discontinuous yielding at the yield point and is evidenced by irregular striations on the surface of the sheet. The second type of stretcher strain marking is caused by discontinuous yielding in the plastic region of the material and is evidenced by regular striations on the surface of the sheet **[19].**

3.5.5 Springback

In addition to the formability concerns, sprinback is another significant problem that must be solved in order to form the exact shape of the product.Sprinback is a common phenomenon in sheet metal forming and can be affected by various parameters such as material properties, tooling geometry,friction between the sheet metal and the tooling,blank holder force,etc.As soon as the deformed part removed from the die cavity, springback occurs,espicially where bending,unbending and bending-unbending-reverse bending are performed. Change in shape that caused by sprinback introduces problems in assebly process, so die makers must allow for the sprinback before having troubles **[4].**

Finite element method takes place again in order to predict sprinback in the die design stage. General tendency on springback phenomenon is passing a little work to do for the tool operators who are finalize the die making job. In this view, experince and knowledge of the FEM user is very significant here. Considering which hardening rule is accounted for, yielding criteria selected, behaviours of the materials and which operations will be applied during the process help the work to do easier.

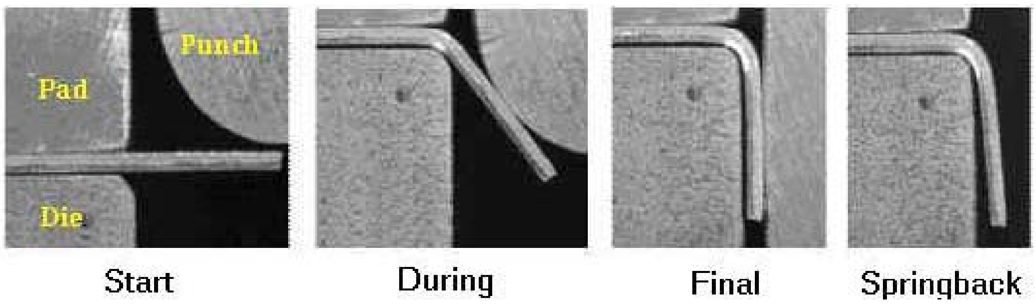

Figure 3.10: Springback evolution

Furthermore, the accuracy of this unloading bending moment depends on the internal stress distribution within the sheet metal element.In other words, it is not possible to obtain an accurate sprinback prediction with a rough internal stress disribution. Most of the sheet materials undergo complicated deformation histories during the forming process.This means that the Bauschinger effect exists within these elements since they may have one or more reverse yields. Therefore, The Bauschinger effect has to be considered for obtaining an accurate internal stress distribution within the sheet metal **[4].**

3.6 Effects of Properties on Forming

It is found that the way in which a given sheet behaves in a forming process will depend on one or more general characteristics. Which of these is important will depend on the particular process and by studying the mechanics equations governing the process it is often possible to predict those properties that will be important. This assumes that the property has a fundamental significance, but, not all the properties obtained from the tensile test will fall into this category. The general attributes of material behaviour that affect sheet metal forming are as follows **[1].**

3.6.1 Shape of the true stress-strain curve

The important aspect is strain-hardening. The greater the strain-hardening of the sheet, the better it will perform in processes where there is considerable stretching; the straining will be more uniformly distributed and the sheet will resist tearing when strain-hardening is high. There are a number of indicators of strain-hardening and the strain-hardening index, *n*, is the most precise. Other measures are the tensile/yield ratio, the total elongation, and the maximum uniform strain, the higher these are, the greater is the strain-hardening.

The importance of the initial yield strength, is related to the strength of the formed part and particularly where lightweight construction is desired, the higher the yield strength, the more efficient is the material. Yield strength does not directly affect forming behaviour, although usually higher strength sheet is more difficult to form. This is because of other properties change in an adverse manner as the strength increases. The elastic modulus also affects the performance of the formed part and a higher modulus will give a stiffer component, which is usually an advantage. In terms of forming, the modulus will affect the springback. A lower modulus gives a larger springback and usually more difficulty in controlling the final dimensions. In many cases, the springback will increase with the ratio of yield stress to modulus, and higher strength sheet will also have greater springback [1].

3.6.2 Anisotropy

If the magnitude of the planar anisotropy parameter, ΔR, is large, either, positive or negative, the orientation of the sheet with respect to the die or the part to be formed will be important; in circular parts, asymmetric forming and earing will be observed. If the normal anisotropy ratio R is greater than unity it indicates that in the tensile test the width strain is greater than the thickness strain; this may be associated with a greater strength in the through-thickness direction and, generally, a resistance to thinning. Normal anisotropy R also has more subtle effects. In drawing deep parts, a high value allows deeper parts to be drawn. In shallow, smoothly-contoured parts such as autobody outer panels, a higher value of R may reduce the chance of wrinkling or ripples in the part. Other factors such as inclusions, surface topography, or fracture properties may also vary with orientation; these would not be indicated by the R- value which is determined from plastic properties [1, 14].

3.6.3 Fracture

Even in ductile materials, tensile processes can be limited by sudden fracture. The fracture characteristic is not given by total elongation but is indicated by the cross-sectional area of the fracture surface after the test-piece has necked and failed. This is difficult to measure in thin sheet and consequently problems due to fracture may not be properly recognized [1].

3.6.4 Homogeneity

Industrial sheet metal is never entirely homogeneous, nor free from local defects. Defects may be due to variations in composition, texture or thickness, or exist as point defects such as inclusions. These are difficult to characterize precisely. Inhomogeneity is not indicated by a single tensile test and even with repeated tests, the actual volume of material being tested is small, and non-uniformities may not be adequately identified [1].

3.6.5 Surface Effects

The roughness of sheet and its interaction with lubricants and tooling surfaces will affect performance in a forming operation, but will not be measured in the tensile test. Special tests exist to explore surface properties [1].

3.6.6 Damage

During tensile plastic deformation, many materials suffer damage at the microstructural level. The rate at which this damage progresses varies greatly with different materials. It may be indicated by a diminution in strain-hardening in the tensile test, but as the rate of damage accumulation depends on the stress state in the process, tensile data may not be indicative of damage in other stress states [1].

3.6.7 Rate Sensivity

The rate sensitivity of most sheet is small at room temperature; for steel it is slightly positive and for aluminium, zero or slightly negative. Positive rate sensitivity usually improves forming and has an effect similar to strain-hardening. As well as being indicated by the exponent m, it is also shown by the amount of extension in the tensile test-piece after maximum load and necking and before failure [1].

4. HARDENING MODELS AND CONSTITUTIVE EQUATIONS

4.1 Introduction

Sheet metal forming is a difficult job that makes the engineers and operators to struggle until the desired part is obtained. Sheet metal processes involve design stage, material selections, forming simulations using computer codes or commercial softwares which are said to be die design, blank design, stamping, trimming, flanging simulations etc. These processes continue with the try-outs until the dimensions of the part remain in the specified tolerances. All these operations can go up to the time interval of 12 – 15 months.

It is obvious that any mistake in these time-consuming operations cause loss of money for die makers and patience and confident of the customer.

As a result, the parameters have great importance which are used in simulations for predicting exact data with minimum time and material loss.

In this section, one can find the basic concepts of sheet metal forming and also some critical points which engineers must pay attention about the usage of yielding criteria.

4.2 Isotropy Of The Materials

A metal, in its generally used form, is a compact aggregate of crystal grains with varying shapes and orientation, each grain having grown from a separate nucleus in the melt. The metal may be considered macroscopically isotropic when the orientations are randomly distributed and when the average dimensions of the individual crystals are small compared with the dimensions of whole specimen. Nevertheless the properties of an aggregate are not always simply statistical averages of the properties of a single crystal, taken over all orientations. While this is approximately true of properties which depend mainly on the bulk structure, such as the coefficient of thermal expansion or the elastic moduli, it is not necessarily true of the plastic phenomena [7].

Shortly, If there is no difference in the metal's microstructure in all directions, the metal is said to be isotropic.

4.3 Anisotropy Of The Materials

The microstructure of metallic materials can be either isotropic or anisotropic. This means that the microstructure can be either constant in all directions or be aligned in a certain direction. If the metal has any pattern or alignment of its microstructure, it is said to be anisotropic. Anisotropy is considered in two forms; normal and planar. Normal anisotropy measures the change in material characteristics, which differ through the thickness of the sheet, while planar anisotropy measures material characteristic differences in various directions within the plane of the sheet. Figure 4.1 defines normal and planar anisotropy relative to the sheet [14].

The microstructure of the metal can have great impact on the ability of the metal to be formed into the desired shape. A prevalent cause for planar anisotropy in sheet metals is the rolling direction. During processing of sheet metal, the rolling operation elongates and aligns the grains of the metal's microstructure in the rolling direction and packs the grains in the thickness direction, which leads to significantly different strength properties within the material.

The internal stress state at the end of forming depends on the plastic properties of the material and their evolution during forming. Cold-rolling induces preferred orientation of polycrystalline grains, and the texture-induced anisotropy can be assessed by measured plastic anisotropy parameters related to strains (r-values) or flow stresses, or can be predicted from texture measurements using simple averaging rules [21].

During a tensile test, the width of the material and the thickness decrease as the elongation increases. The plastic strain ration, r, is the ratio of width strain to thickness strain.

$$r = \frac{\varepsilon_w}{\varepsilon_t} \qquad \textbf{(4.1)}$$

Where ε_w is the width strain and ε_t is the thickness strain. This ratio is useful for determining the degree of anisotropy in the material and rating its resistance to thinning. If the ratio is equal to one, then the material is isotropic, since the strain is equal in both thickness and width. The r ratio values are a measure of the drawability of the sheet metal [16].

For high strain ratios, the material is said to be resistant to thinning, while materials with low strain ratios will be undesirable for forming operations, since it will thin and possibly rupture.

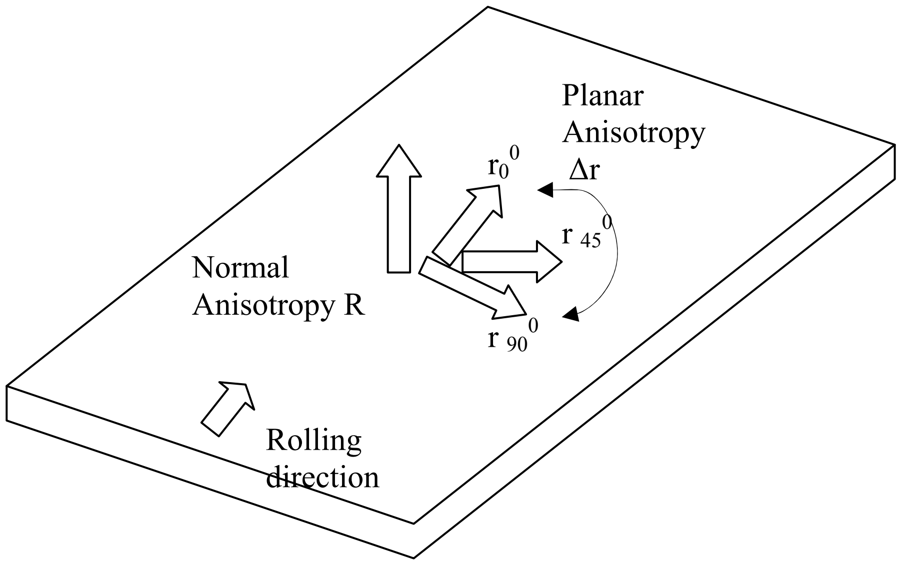

Figure 4.1: Sheet orientation relative to normal and planar anisotropy [14].

The strain ratio is determined relative to the rolling direction of the sheet material, thus r_0 (parallel), r_{45} (diagonal) and r_{90} (transverse) can be determined through geometry. The plastic anisotropy coefficients are assessed by the means of plastic strain ratios of these three planes which are also called as Lankford coefficients. The weighted average, R, of these strain ratios, which is also called normal anisotropy is defined as

$$R = \frac{r_0 + 2r_{45} + r_{90}}{4} \qquad \textbf{(4.2)}$$

The directional strain ratio measures are useful for determining the earing tendency of the material, Δr [14, 25].

$$\Delta r = \frac{r_0 - 2r_{45} + r_{90}}{2} \quad \textbf{(4.3)}$$

Where Δr is the earing tendency, r_0, r_{45}, and r_{90} are the strain ratios. The Earing tendency is simply the likelihood that the sheet will draw non uniformly and form ears in the flange [14].

4.4 Strain Rate

During deformation, material flow is rarely uniform in all directions and regions. The velocity of the metal flow depends on the geometry of the die, strain hardening, temperature, material microstructure, anisotropy, and applied loading rate.

The velocity of metal flow is described as

$$v = \frac{\partial u}{\partial t} \quad \textbf{(4.4)}$$

Where v is the deformation velocity, u is the displacement of material, and t is a measure of time. Metal flow is not necessarily the same in all directions within the material, thus, flow velocity has directional components v_x, v_y, and v_z

$$v_x = \frac{\partial u_x}{\partial t} \;,\quad v_y = \frac{\partial u_y}{\partial t} \;,\quad v_z = \frac{\partial u_z}{\partial t} \quad \textbf{(4.5)}$$

Strain rate is defined as the change in strain with respect to time. Since strain is dependent on the deformation of the material with respect to distance, strain rate can be defined as the change in metal flow with respect to change in location **[14].**

$$\dot{\varepsilon}_x = \frac{\partial \varepsilon_x}{\partial t} = \frac{\partial}{\partial t}\frac{\partial u_x}{\partial x} = \frac{\partial}{\partial x}\frac{\partial u_x}{\partial t} \Rightarrow \dot{\varepsilon}_x = \frac{\partial v_x}{\partial x} \quad \textbf{(4.6)}$$

Where $\dot{\varepsilon}_x$ is the strain rate, u is the deformation of material, v is the deformation velocity and t is a measure of time. The strain rate values in the other directions, are derived in a similar manner.

$$\dot{\varepsilon}_y = \frac{\partial v_y}{\partial y} \quad \textbf{(4.7)}$$

$$\dot{\varepsilon}_z = \frac{\partial v_z}{\partial z} \quad \textbf{(4.8)}$$

Shear strain rate is defined as

$$\dot{\gamma}_{xy} = \frac{\partial v_x}{\partial y} + \frac{\partial v_y}{\partial x} \quad \textbf{(4.9)}$$

Where $\dot{\gamma}_{xy}$ is the shear strain rate and v is the deformation velocity. As with normal strain rate, shear strain rate has components $\dot{\gamma}_{yz}$ and $\dot{\gamma}_{xz}$ defined similar to $\dot{\gamma}_{xy}$.

$$\dot{\gamma}_{yz} = \frac{\partial v_y}{\partial z} + \frac{\partial v_z}{\partial y} \qquad \textbf{(4.10)}$$

$$\dot{\gamma}_{xz} = \frac{\partial v_x}{\partial z} + \frac{\partial v_z}{\partial x} \qquad \textbf{(4.11)}$$

The state of deformation in a plastically deforming metal can be fully described by the displacements, u, velocities, v, strains, ε, and strain rates, $\dot{\varepsilon}$. These values can be defined in an auxiliary coordinate system (x',y',z') if the angle of rotation form the global coordinate system (x,y,z) is known. Thus, a small element in the deforming body can be oriented such that it is not subjected to shear. With this definition, the shear strains, γ_{xy}, γ_{yz} and γ_{xz}, equal zero and the element deforms along the principle axes. This representation of deformation corresponds with the results of uniaxial tension tests, since they also deform in the principal direction.

The assumption of volume constancy neglects elastic strain when the relative plastic strain is much greater. This assumption can also be expressed, for deformation along principle axes, as follows:

$$\varepsilon_x + \varepsilon_y + \varepsilon_z = 0 \qquad \textbf{(4.12)}$$

$$\dot{\varepsilon}_x + \dot{\varepsilon}_y + \dot{\varepsilon}_z = 0 \qquad \textbf{(4.13)}$$

Strain and strain rate, along with temperature, affect the magnitude of the flow. This relationship is usually dependent on the direction of the strain (anisotropy), because the properties of a sheet material (i.e. flow stress as a function of strain, strain rate, and temperature) depend on the rolling direction.

4.5 True and Engineering Strains

Strength of materials theory defines engineering strain as deformation with respect to the initial length, thus:

$$e = \frac{\lambda_f - \lambda_0}{\lambda_0} \quad \textbf{(4.14)}$$

where e is the engineering strain, λ_f is the deformed length and λ_0 is the original length. This measure of strain is useful for design, since it is very easy to calculate. Engineering strain is not accurate for large deformations, however for design purposes, the component is assumed to deform very little, so this measure provides useful results [14].

For large deformations, more accurate measure of deformation is true strain, which relates the change in length to instantaneous unit length. Instantaneous true strain is defined as:

$$\varepsilon = \int_{\lambda_0}^{\lambda_f} \frac{d\lambda}{\lambda} = \ln\left(\frac{\lambda_f}{\lambda_0}\right) \quad \textbf{(4.15)}$$

where ε is the true strain, λ_f is the deformed length, and λ_0 is the original unit length. This measure provides the exact value of strain, taking into account the effects of dimensional change. True strain is useful when large deformations occur, such as forming operations thus it is commonly used for process design.
Engineering and true strains are related by the following equation

$$\varepsilon = \ln(e+1) \quad \textbf{(4.16)}$$

This equation provides an easy conversion from engineering to true strain depending on available information.

4.6 Yield Criteria

The analysis of localized necking is strongly dependent on the yield function. Since the geometric configuration of the yield surface has a significant influence on predicted forming limit strains, many yield criteria have been proposed to reflect the material properties of sheet metals. Usage of these criteria are vary with different kinds of materials and different loading conditions. By these considerations, better simulation results will be obtained.

The common yield criteria are listed below:

4.6.1 Tresca Criterion

Based on Coulomb's results on soil mechanics and his own experiments results on the metal extrusion, Tresca (1864) proposed a yield criterion, and this criterion can be expressed as

$$Max\left[\frac{1}{2}|\sigma_1 - \sigma_2|, \frac{1}{2}|\sigma_2 - \sigma_3|, \frac{1}{2}|\sigma_1 - \sigma_3|\right] = k \quad \textbf{(4.17)}$$

Where k value can be determined by the uniaxial test, and its value is equal to a half of the yield stress.

4.6.2 Von Mises Yield Criterion

Von Mises (1913) yield criterion, which can also be called a J_2 criterion, can be written as:

$$(\sigma_1 - \sigma_2)^2 + (\sigma_2 - \sigma_3)^2 + (\sigma_3 - \sigma_1)^2 = 2\sigma_y^{\ 2} \quad \textbf{(4.18)}$$

$$S_{ij}S_{ij} = \frac{2}{3}\sigma_y^{\ 2} \quad \textbf{(4.19)}$$

Where Sij and σ_y are the deviatoric stress tensor and yield stress, respectively.

4.6.3 Hosford's Generalized Isotropic Yield Criterion

Hershey (1954) and Hosford (1972) proposed the generalized isotropic yield criterion based on the results of polycrystalline calculations. The formulation is expressed in principal stresses, and high order exponents are found to be crystal structure-related typically 6 for BCC and 8 for FCC metals [23] which is shown in the equation 4.20.

$$\left[\frac{(\sigma_1-\sigma_2)^M+(\sigma_2-\sigma_3)^M+(\sigma_1-\sigma_3)^M}{2}\right]^{1/M}=Y \qquad \textbf{(4.20)}$$

Where $(\sigma_1 \geq \sigma_2 \geq \sigma_3)$ and $(1 \leq M \leq \infty)$ is proposed

When M = l, the above equation becomes Tresca criterion, and becomes Von Mises criterion if M = 2. Because it repeats its shape at lower values when M > 2.767, the above equation becomes Tresca and Von Mises criteria when M = ∞ and 4 respectively [4].

Hosford later modified the formula for plane stress conditions and tried to accommodate shear stresses [23, 27].

4.6.4 Hill's 48 Yield Criterion

Hill proposed several yield criterials which are used for different materials and different situations.Theory of Hill (1948-1950) describes a state of simple orthotropic anisotropy, that is, where there are three mutually orthogonal planes of symmetry at every point. The intersections of these planes are known as the principal axes of anisotropy [13, 29].

$$\begin{aligned} 2f(\sigma_{ij}) &= F(\sigma_y-\sigma_z)^2+G(\sigma_z-\sigma_x)^2+H(\sigma_x-\sigma_y)^2+2L\tau^2{}_{yz} \\ &+2M\tau^2{}_{zx}+2N\tau^2{}_{xy}=1 \end{aligned} \qquad \textbf{(4.21)}$$

The coefficients of F, G, H, N are calculated by r_0, r_{45}, r_{90} are the tensile test strain ratios in rolling, diagonal and transverse directions, respectively [12].

$$F=\frac{R_0}{R_{90}(1+R_0)} \qquad \textbf{(4.22)}$$

$$G=\frac{1}{1+R_0} \qquad \textbf{(4.23)}$$

$$H=\frac{R_0}{1+R_0} \qquad \textbf{(4.24)}$$

$$N = \frac{(R_0 + R_{90})(1 + 2R_{45})}{2R_{90}(1 + R_0)} \quad \textbf{(4.25)}$$

For sheet metal forming process, plane stress assumption is adopted and the above equation can be simplified by setting [4]

$$\sigma_z = \sigma_{xy} = \sigma_{yz} = 0 \quad \textbf{(4.26)}$$

Recalling $\bar{R}$ is normal anisotropy from equation 4.2, equation 4.26 can be rewritten by considering sheet metal forming and assuming that the sheet has planar isotropy where σ_u is the in-plane uniaxial tensile stress [8].

$$\sigma^2{}_1 + \sigma^2{}_2 + \bar{R}(\sigma_1 - \sigma_2)^2 = \left(1 + \bar{R}\right)\bar{\sigma}^2{}_u \quad \textbf{(4.27)}$$

Hill's quadratic yield function has been used in various analyses of metal forming processes to account for polycrystalline texture.It is formulated in a general stress state, and needs only uniaxial tensile tests to describe planar anisotropy. Hovewer, it is not very suitable for FCC metals exhibiting low R-values, such as aluminum alloy sheets **[23].**

In the application chapter, the effect of R-values shown using Hill48 yield criteria.

4.6.5 Hill's 79 Criterion

For aluminum sheet, the r-value is normally less than unity (between 0.6 and 0.8). Experimental data show that for most aluminum sheet the yield stress for balanced biaxial tension is larger than the yield stress for uniaxial tension (anomalous behavior). Therefore, eq. (4.37) contradicts the physical phenomenon of aluminum sheets. This indicates that the 1948 criterion may encounter problems when predicting forming limits of aluminum. In order to deal with the anomaly, Hill proposed the second yield criterion in 1979 which is a generalization of the Logan and Hosford yield Criterion [8, 9, 27].

$$\begin{aligned} F|\sigma_2 - \sigma_3|^m + G|\sigma_3 - \sigma_1|^m + H|\sigma_1 - \sigma_2|^m + A|2\sigma_1 - \sigma_2 - \sigma_3|^M \\ + B|2\sigma_2 - \sigma_3 - \sigma_1|^M + C|2\sigma_3 - \sigma_1 - \sigma_2|^M = 2\sigma^m \end{aligned} \quad \textbf{(4.28)}$$

There are 7 parameters in eq. (4.28). They are determined by uniaxial tension test in the three orthotropic directions, together with three transverse strain ratios, plus 1 other combined loading test (such as the biaxial tension test). For in-plane isotropy, the four simple forms of eq. (4.29) were given by Hill and the yield locus of the fourth equation remains convex as long as the exponent M is greater than unity Using both uniaxial tension yield stress σ_u and r-value, the fourth equation becomes as below [8].

$$|\sigma_1 + \sigma_2|^M + (1+2r)|\sigma_1 - \sigma_2|^M = 2(1+r)\sigma_u{}^M \quad \textbf{(4.29)}$$

Calculation of *M* value is made by fitting of work hardening curves for equi-biaxial stretching calculated on the base of experimentally determined work hardening curves in tensile test to experimentally determined work hardening curves in equibiaxial stretching. It is well knowthat the Hill’79 can model the Woodthorpe–Pearce “anomalous” behavior of some materials but the main disadvantage is that it is expressed using only principal stress and the predicted yield surfaces are sometimes far from the experimental surfaces predicted by the Bishop–Hill theory [6].

4.6.6 Hill’s 1990 Yield Criterion

Hill’s 90 Criterion Coefficients: are α, β, γ and m. The anisotropic elasto-plastic plane stress formulation of shell material type is based on a non-quadratic yield function (Hill 1990), as opposed to a quadratic yield function (Hill 1948). For plane stress conditions and in the orthotropic axes, the yield function is written as equation 4.30 [31].

$$\begin{aligned} &|(\sigma_{11} + \sigma_{22})|^m + \alpha^m\left[(\sigma_{11} - \sigma_{22})^2 + 4\sigma^2{}_{12}\right]^{\frac{m}{2}} + \left[\sigma_{11}{}^2 + \sigma_{22}{}^2 + 2\sigma^2{}_{12}\right]^{\frac{m}{2}-1} \\ &\left\{\beta\left(\sigma_{11}{}^2 - \sigma_{22}{}^2\right) + \gamma(\sigma_{11} - \sigma_{22})^2\right\} = \\ &= \left(1 + \alpha^m + \beta + \gamma\right)(\sigma_{22})^m = \left(2\sigma^b{}_y\right)^m \end{aligned} \quad \textbf{(4.30)}$$

Table 4.1: Hill 90 parameters

Properties	Symbol
material dependent data	α, β, γ and m
yield stress under uni-axial tension on rolling direction	σ22
yield stress under equi-biaxial tension	σ by

4.6.7 Hill's 1993 Yield Criterion

The yield function proposed by Hill in 1993 is in equation 4.31 where c, p and q are non-dimensional parameters given by equations 4.32 and 4.33

$$\frac{\sigma_1^{\,2}}{\sigma_0^{\,2}} - \frac{c\sigma_1\sigma_2}{\sigma_0\sigma_{90}} + \frac{\sigma_2^{\,2}}{\sigma_{90}^{\,2}} + \left[(p+q) - \frac{p\sigma_1 + q\sigma_2}{\sigma_b}\right] - \frac{\sigma_1\sigma_2}{\sigma_0\sigma_{90}} = 1 \qquad \textbf{(4.31)}$$

$$\frac{c}{\sigma_0\sigma_{90}} = \frac{1}{\sigma_0^{\,2}} + \frac{1}{\sigma_{90}^{\,2}} - \frac{1}{\sigma_b^{\,2}} \qquad \textbf{(4.32)}$$

$$\left(\frac{1}{\sigma_0} + \frac{1}{\sigma_{90}} - \frac{1}{\sigma_b}\right)p = \frac{2r_0(\sigma_b - \sigma_{90})}{(1+r_0)\sigma_0^{\,2}} - \frac{2r_{90}\sigma_b}{(1+r_{90})\sigma_{90}^{\,2}} + \frac{c}{\sigma_0}$$
$$\left(\frac{1}{\sigma_0} + \frac{1}{\sigma_{90}} - \frac{1}{\sigma_b}\right)q = \frac{2r_{90}(\sigma_b - \sigma_0)}{(1+r_{90})\sigma_{90}^{\,2}} - \frac{2r_0\sigma_b}{(1+r_0)\sigma_0^{\,2}} + \frac{c}{\sigma_{90}} \qquad \textbf{(4.33)}$$

In the above equations, σ_0 and σ_{90} yield stresses for uniaxial tension at 0^0 and 90^0 to the rolling direction respectively and r_0 and r_{90} are ratios of transverse to through-thickness strain corresponding to σ_0 and σ_{90} respectively. Similar to the definition of σ_b, it is assumed that the ratio of the yield stresses σ_u and σ_{90} also remains constant so that . Then eqs. (4.32) and (4.33) are written as

$$\frac{\sigma_1^{\,2}}{\sigma_0^{\,2}} - \alpha_0\frac{c\sigma_1\sigma_2}{\sigma_0^{\,2}} + \alpha_0^{\,2}\frac{\sigma_2^{\,2}}{\sigma_0^{\,2}} + \alpha_0\left[(p+q) - \sigma_b\frac{p\sigma_1 + q\sigma_2}{\sigma_0}\right]\frac{\sigma_1\sigma_2}{\sigma_0^{\,2}} = 1 \qquad \textbf{(4.34)}$$

Where

$$c = \frac{1}{\sigma_0} + \alpha_0 - \frac{\alpha_b^{\,2}}{\alpha_0} \qquad \textbf{(4.35)}$$

$$(1+\alpha_0 - \alpha_b)p = \frac{2r_0(\alpha_0 - \alpha_b)}{(1+r_0)\alpha_0\alpha_b} - \frac{2r_{90}\alpha_0^{\,2}}{(1+r_{90})\alpha_b} + c$$
$$(1+\alpha_0 - \alpha_b)q = \frac{2r_{90}(1-\alpha_b)\alpha_0^{\,2}}{(1+r_{90})\alpha_b} - \frac{2r_0}{(1+r_0)\alpha_b} + \alpha_0 c \qquad \textbf{(4.36)}$$

It is noted that if $\alpha_{0,}$ α_b r_0 r_{90} are all selected to be unity, equation becomes the von Mises yield criterion. It is also interesting to point that in the case of in-plane isotropy, Hill's 1993 and the 1979 yield functions (eqs. (4.34) and (4.31)) reduce to his 1948 yield function if σ_b is determined from eq. 4.37

$$\sigma_b = \sqrt{\frac{r+1}{2}}\sigma_u \qquad \textbf{(4.37)}$$

4.6.8 Barlat and Lian's Yield Critetion

Another non-quadratic yield criterion proposed by Barlat and Lian (1989) included a shear stress term in the expression of the effective stress, and this criterion made it possible to predict the plastic behavior for the complete range of strain ratios without the trouble which may occur by using Hill's 1979 or Hosford's 1979 yield function. This yield condition was for the three-dimensional plane stress case, which is often assumed in sheet forming problems [30].

$$\alpha\left|K_1 + K_2\right|^m + \alpha\left|K_1 - K_2\right|^m + (2-\alpha)\left|K_2{}^m\right| = 2\overline{\sigma}^m \qquad \textbf{(4.38)}$$

$$K_1 = \frac{\sigma_{xx} + h\sigma_{yy}}{2}$$
$$K_2 = \sqrt{\left(\frac{\sigma_{xx} + h\sigma_{yy}}{2}\right)^2 + p^2\sigma_{xy}{}^2} \qquad \textbf{(4.39)}$$

where K1 and K2 were modified stress tensors, α, h, p and m were material constants, and $\overline{\sigma}$ was effective stress.

5. APPLICATIONS

5.1 Introduction

The physical mechanisms of forming processes like deep drawing are highly complex due to the non-linear behaviour of elasto-plasticity theory leading to a complex interaction of sophisticated product geometries in three dimensions and with respect to time. Theoretical descriptions for a better understanding are difficult as the sub-mechanisms can often not be separated or localized. However, proper product design, tolerances and quality demand for suitable tool development, corresponding to high costs and large lead times. Therefore in the field of sheet metal forming numerical simulation tools usually based on the Finite Element Method (FEM), have become more and more common in the development process. They enable to predict how the press tools and parameters should be designed to achieve the optimum shape of the sheet metal components, thus substantially reducing the number of experimental trials. During this period of time the precision of the simulation tools has increased.

Numerical simulations considered in this thesis will be based on the finite element method. The FE models are presented via two commercial FEA software codes, namely Pam-Stamp 2G and Autoform 4.04.

Formability results are presented with model which run with orthotropic Hill48 yield function.Beside this, isotropic FE model using Von Mises yield fuction and orthotropic Hill 90 yield function are also presented. Regarding the results, a comparison between isotropic and anisotropic materials and a comparison between two different anisotropic yield criterion could be made.

5.2 Process parameters

Proceses parameters are the variables that effect directly to the formability characteritics. In the try-out stage, one of these parameters are changed sligtly while the other kept constant until desired geometry obtained. If, the accurate parameters were figured out, the panel will be ready for the automation.

5.2.1 Material Properties

For the production of the panel Fep05 mild steel is selected which was cold rolled. As a result of rolling, the material becames anisotropic.

Table 5.1: Properties of the material used for panel

Properties	Value
Yield Stress (GPa)	280
Young's Modulus (GPa)	150
Plastic anisotropy parameter, r	2.01
Work-hardening exponent	0.36
Coulomb friction coefficient	0.162
Strength coefficient (GPa)	0.577
Poisson's ratio	0.33
Initial elastic strain component	0.0166
Thickness (mm)	0.75

Table 5.2: Lankford Coefficients of the material

Direction	Value
r0	1.88
r45	1.87
r90	2.43

5.2.2 Mesh Topology

Both Pam-Stamp 2G and Autoform use adaptive mesh as mesh algorithm.When punch touch to the blank, related mesh areas divided to form a finer mesh. This continue until the values that were entered to the software. When geometric stability obtained, related meshes are united to form a coarser mesh which helps to manage more efficiently memory usage. This is called unmesh algorithm and both softwares are using this algorithm.The meshes for the different timesteps are shown below, until the end of the drawing operation.

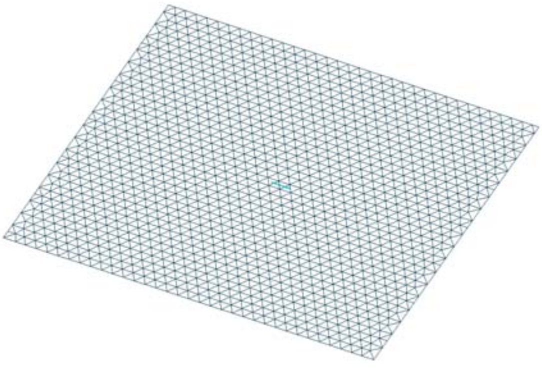

Figure 5.1: Initial mesh for the blank

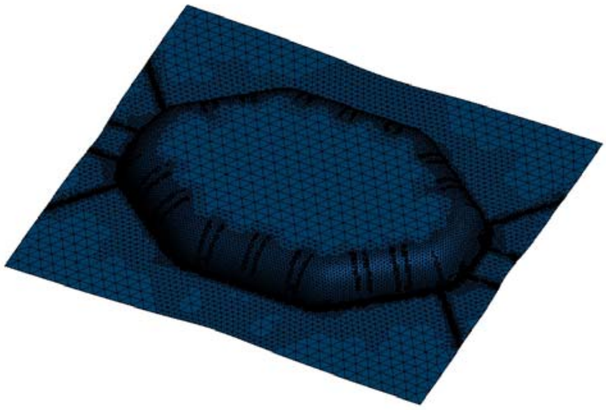

Figure 5.2: Mesh from drawing operation

Figure 5.3: Mesh from the end of drawing operation

5.2.3 Punch Speed

Generally, punch velocity is defined about 1mm/sec, which can be considered as quasi-static speed and as a result of this speed interval, it is not necessary to take the strain rate sensivity for the materials into consideration.

5.2.4 Blank Holder Force

In this process, blank holder force is taken as 100 tonnes. During the evolution of the process, different results were obtained for the different blank holder forces. Finally, 100 tonnes of blank holder force was agreed to be used for the process.

5.2.5 Friction Coefficient

Friction is one of the most important parameter in sheet metal forming operations. Since lubrucation slows down the automation, the goal of all proceses is to obtain the desired geometry without using lubrication.For metal to metal friction, 0.15 friction is taken as a friction coefficient.

5.2.6 Drawbeads

Drawbeads effect is considerable on the formability characteristics as explained in section 3.3. As an important point, the equivalent drawbead force is valuable to mention. In the simulations drawbeads are not simulated as a geometry until resonable solutions are figured out. In the final evolution stage, equivalent drawbead forces replaced by the exact geometries to find out the best geometry which effect the formability in the desired manner.

5.3 Process for the selected panel

At first tool geometries are defined for the simulation. In the simulation program tool geometries are placed in the die coordinates as shown in figure 5.1. After die geometry important from a CAD program, punch is created by an offset operation regarding material thicness and tool offset in the corners. Then additional addenda surfaces are created for the die which are the surfaces that the blank is placed on. As an important point, all fillets or radii must be well defined. In the case of using teoric corners would effect the material slipping and as a result of this, inaccurate results obtained.Also selection of layer in the the tools and in blank is the most common mistake made by the engineers. Offset adjustments must be made by taking the layers in the consideration.

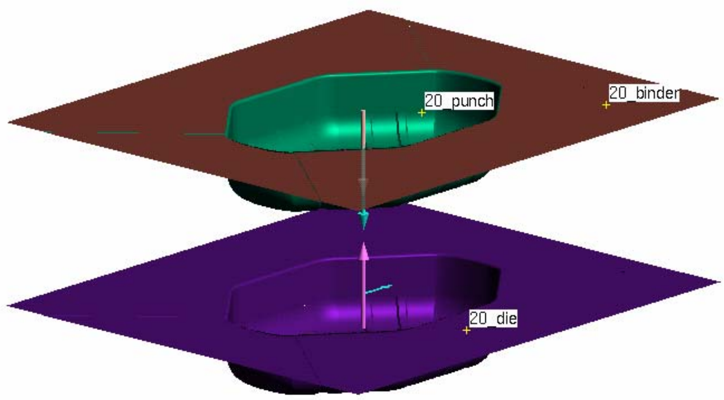

Figure 5.4: Tool geometries

After blank is put on the die, gravity operation is applied. Closing part simulates, binder and blank contact and by this operation blank is hold in exact position and it is then ready for the punch penetration. So drawing operation begins by the moving of punch downwards. Trimming operation is followed after drawing. Springback solution is done for the final stage.

5.4 Results of the drawing simulations respect to variations of Lankford Coefficients

In this section, it is considered to compare the affects of Lankford Coefficients on the formability in a sequence. For this purpose, two different values were used for one of the coefficients while other two coefficients kept constant. Hill 48 yield criterion was used for the solutions. The reasons to use Hill 48 are, need for an anisotropic yield criterion and ease of usage which is only just by changing the coefficients.

$r_0 = 0.5$ $r_{45} = 1.87$ $r_{90} = 2.43$ $r_0 = 2.5$ $r_{45} = 1.87$ $r_{90} = 2.43$

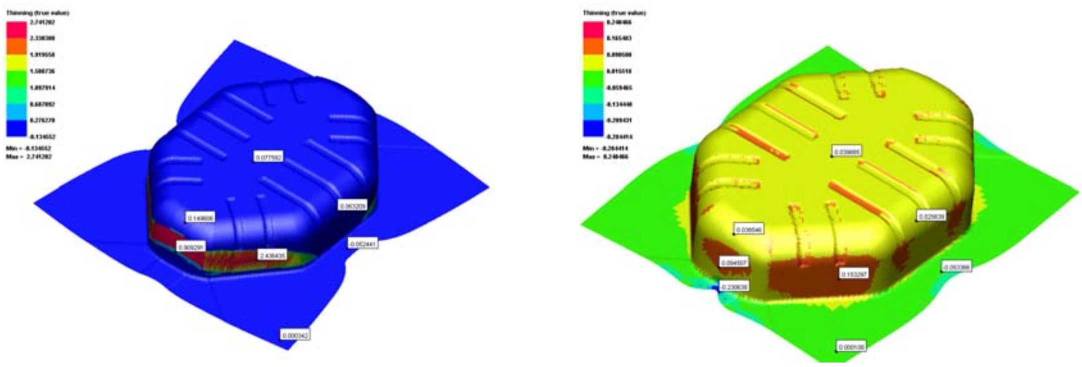

Figure 5.5: Thinning variation with r_0

$r_0 = 1.88$ $r_{45} = 0.5$ $r_{90} = 2.43$ $r_0 = 1.88$ $r_{45} = 2.5$ $r_{90} = 2.43$

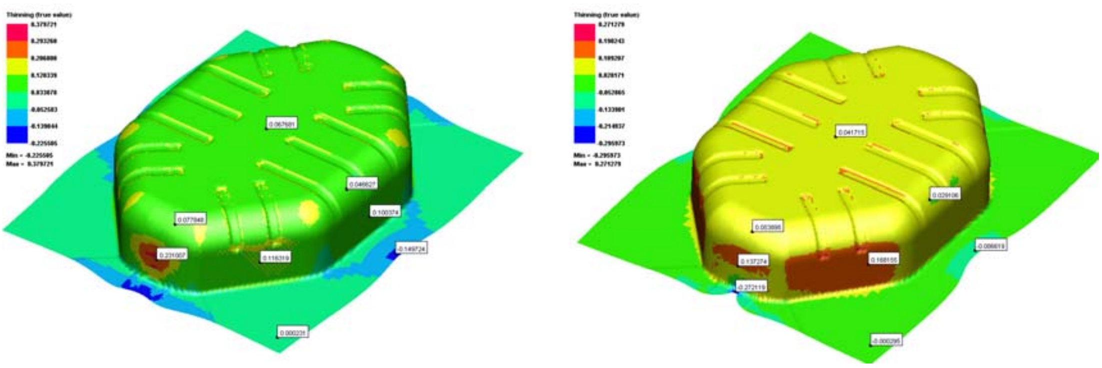

Figure 5.6: Thinning variation with r_{45}

$r_0 = 1.88$ $r_{45} = 1.87$ $r_{90} = 0.5$ $r_0 = 1.88$ $r_{45} = 1.87$ $r_{90} = 3$

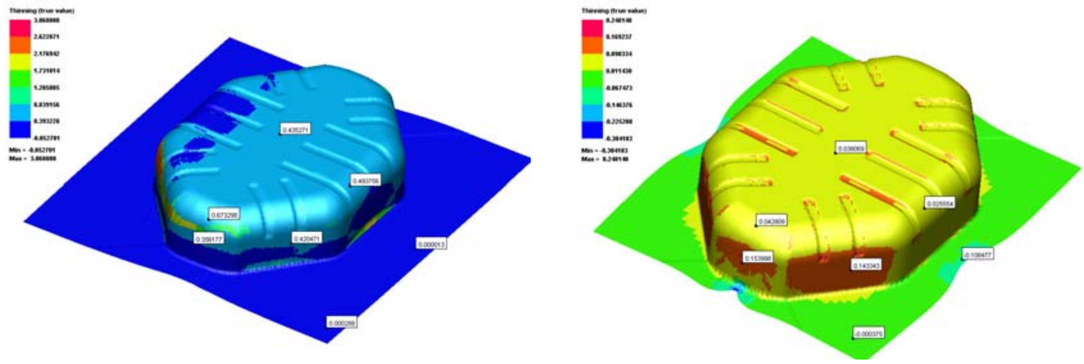

Figure 5.7: Thinning variation with r_{90}

$r_0 = 0.5$ $r_{45} = 1.87$ $r_{90} = 2.43$ $r_0 = 2.5$ $r_{45} = 1.87$ $r_{90} = 2.43$

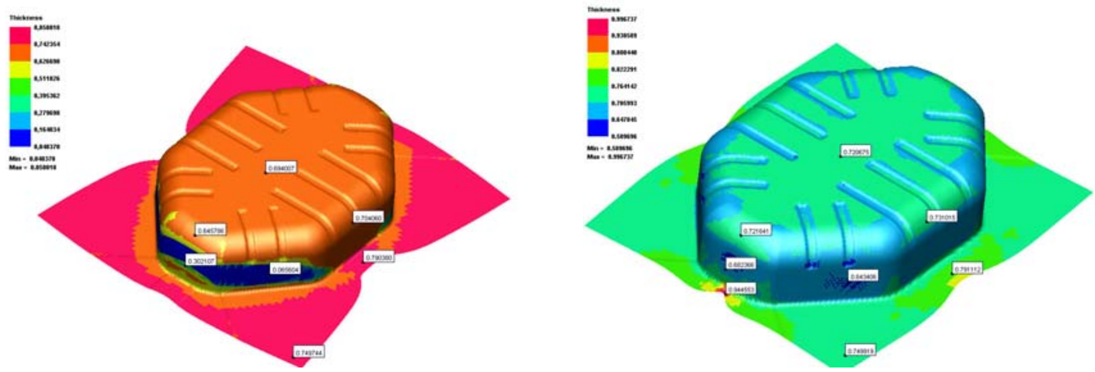

Figure 5.8: Thickness variation with r_0

$r_0 = 1.88$ $r_{45} = 0.5$ $r_{90} = 2.43$ $r_0 = 1.88$ $r_{45} = 2.5$ $r_{90} = 2.43$

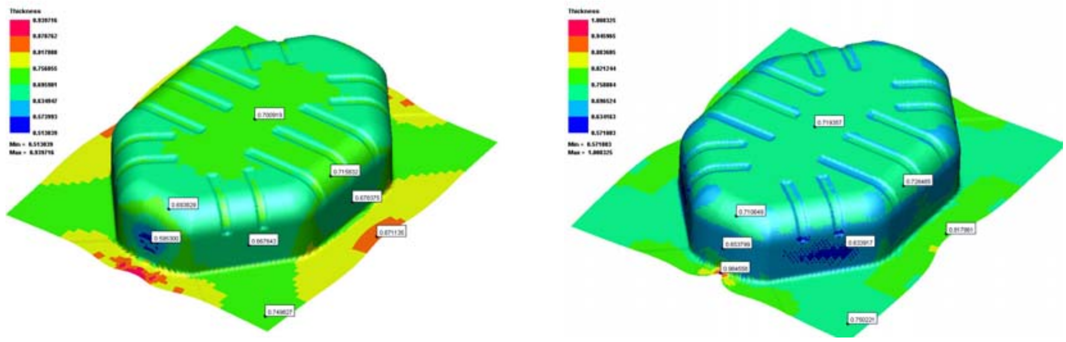

Figure 5.9: Thickness variation with r_{45}

From thinning and thickness results, variation of r_0 and r_{90} affect panel more than than the variation of r_{45}. Generally simulations resulted with a failure after changing these two coefficients.

$r_0 = 1.88$ $r_{45} = 1.87$ $r_{90} = 0.5$ $r_0 = 1.88$ $r_{45} = 1.87$ $r_{90} = 3$

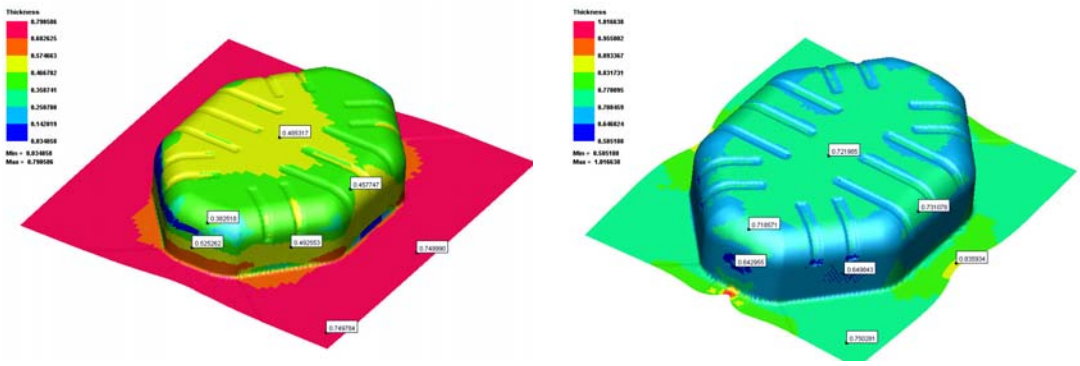

Figure 5.10: Thickness variation with r_{90}

$r_0 = 0.5$ $r_{45} = 1.87$ $r_{90} = 2.43$ $r_0 = 2.5$ $r_{45} = 1.87$ $r_{90} = 2.43$

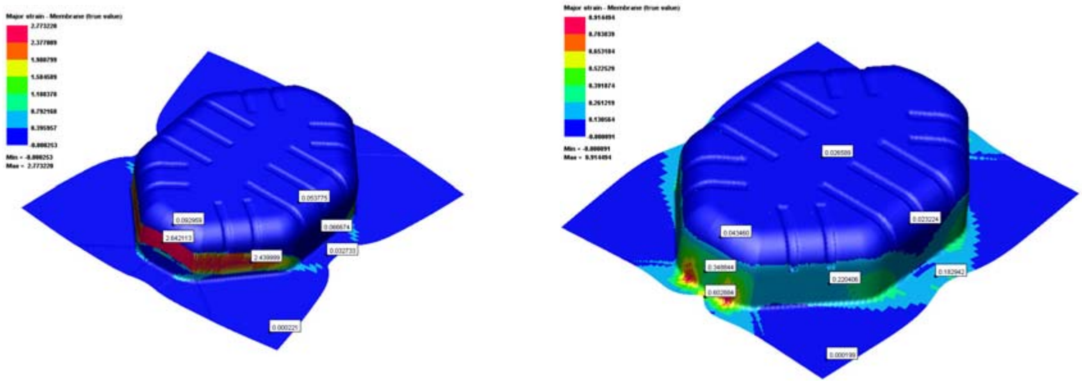

Figure 5.11: Major strain variation with r_0

$r_0 = 1.88$ $r_{45} = 0.5$ $r_{90} = 2.43$ $r_0 = 1.88$ $r_{45} = 2.5$ $r_{90} = 2.43$

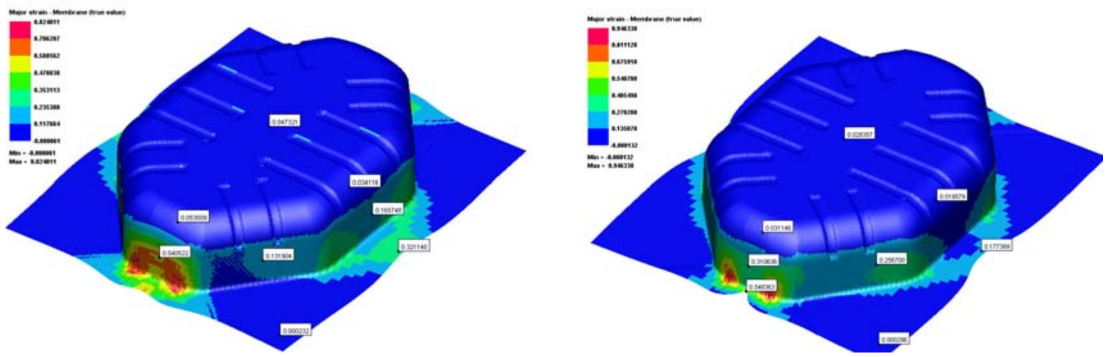

Figure 5.12: Major strain variation with r_{45}

$r_0 = 1.88$ $r_{45} = 1.87$ $r_{90} = 0.5$ $r_0 = 1.88$ $r_{45} = 1.87$ $r_{90} = 3$

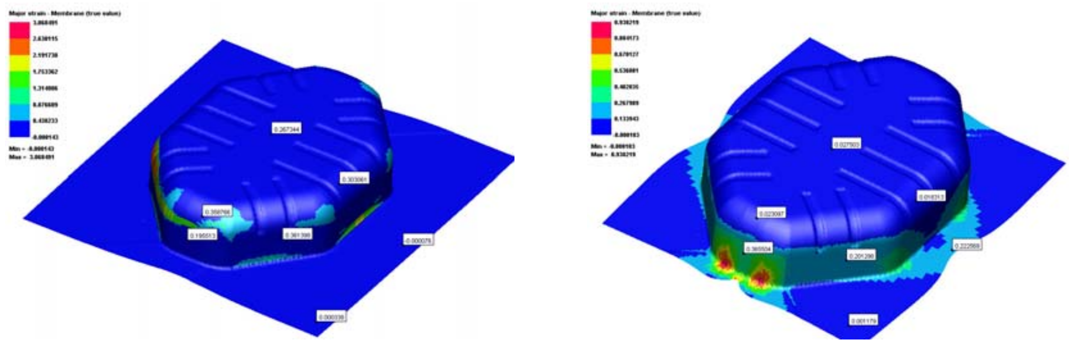

Figure 5.13: Major strain variation with r_{90}

$r_0 = 0.5$ $r_{45} = 1.87$ $r_{90} = 2.43$ $r_0 = 2.5$ $r_{45} = 1.87$ $r_{90} = 2.43$

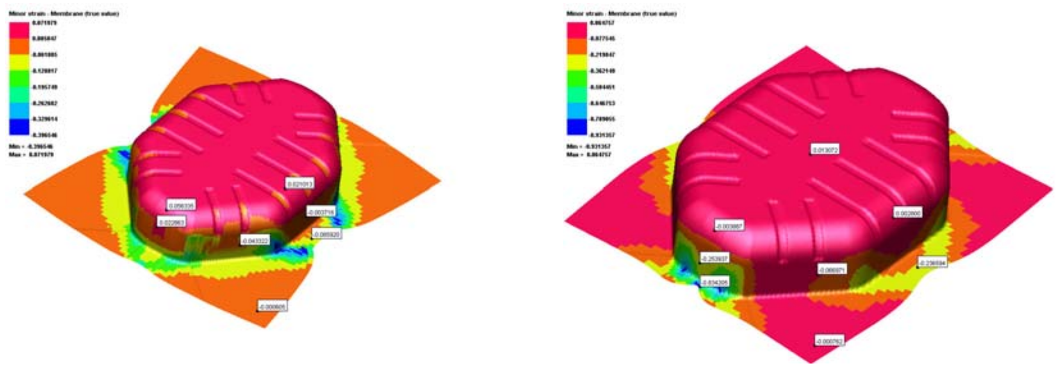

Figure 5.14: Minor strain variation with r_0

$r_0 = 1.88$ $r_{45} = 0.5$ $r_{90} = 2.43$ $r_0 = 1.88$ $r_{45} = 2.5$ $r_{90} = 2.43$

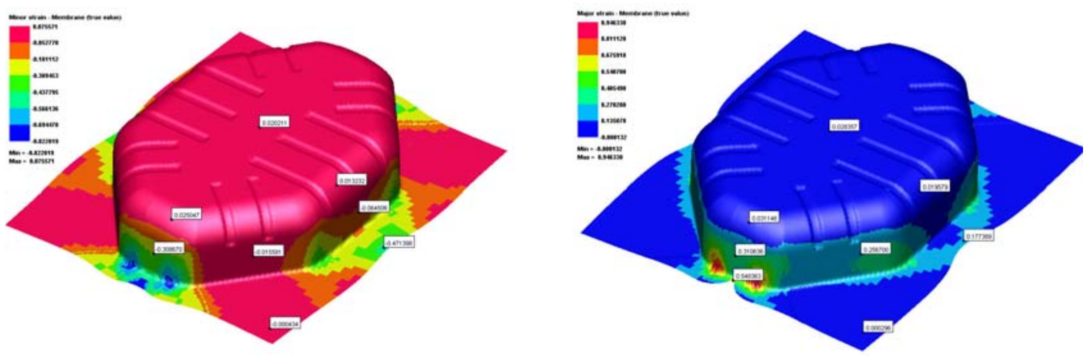

Figure 5.15: Minor strain variation with r_{45}

r_0 = 1.88 r_{45} = 1.87 r_{90} = 0.5 r_0 = 1.88 r_{45} = 1.87 r_{90} = 3

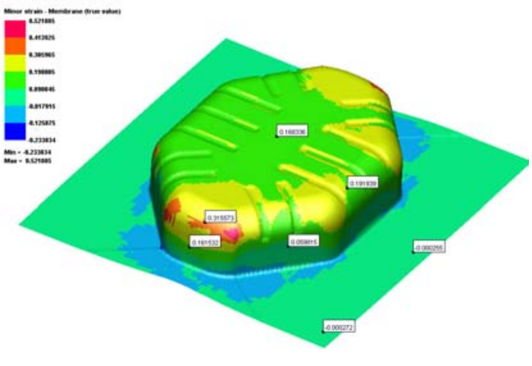

Figure 5.16: Minor strain variation with r_{90}

r_0 = 0.5 r_{45} = 1.87 r_{90} = 2.43 r_0 = 2.5 r_{45} = 1.87 r_{90} = 2.43

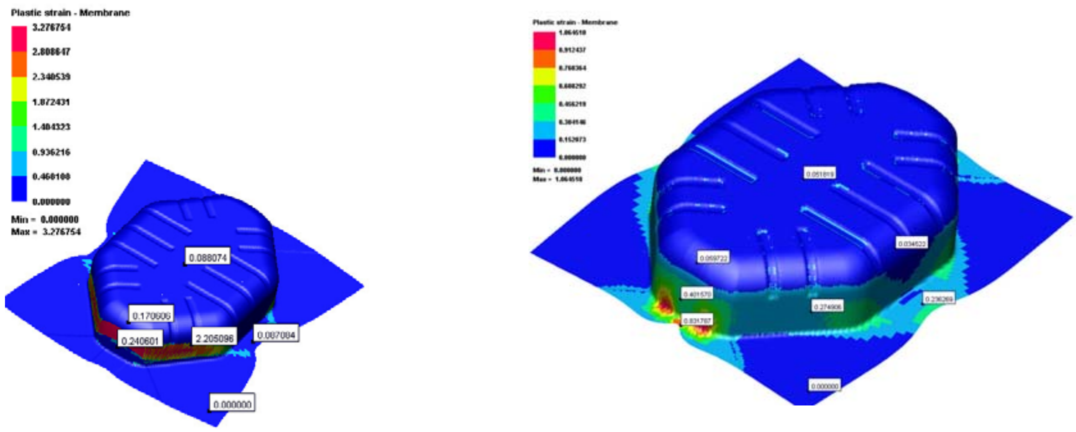

Figure 5.17: Plastic Strain variation with r_0

r_0 = 1.88 r_{45} = 0.5 r_{90} = 2.43 r_0 = 1.88 r_{45} = 2.5 r_{90} = 2.43

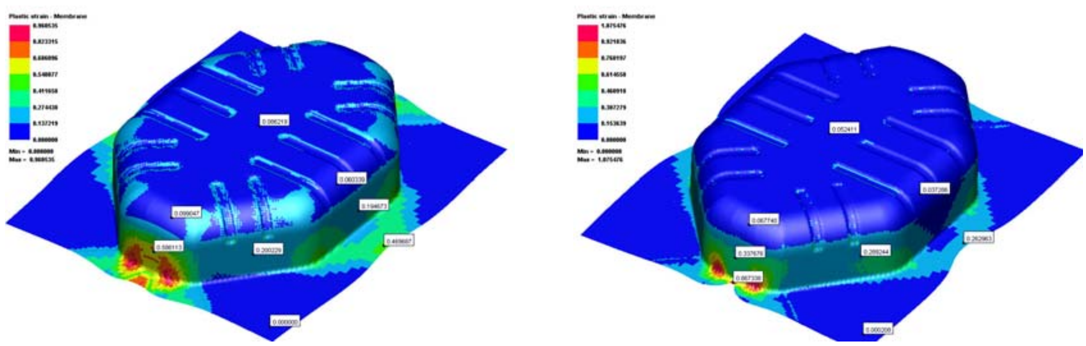

Figure 5.18: Plastic Strain variation with r_{45}

r_0 = 1.88 r_{45} = 1.87 r_{90} = 0.5 r_0 = 1.88 r_{45} = 1.87 r_{90} = 3

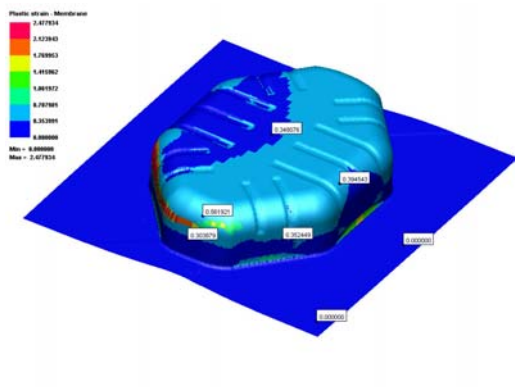

Figure 5.19: Plastic Strain variation with r_{90}

r_0 = 0.5 r_{45} = 1.87 r_{90} = 2.43 r_0 = 2.5 r_{45} = 1.87 r_{90} = 2.43

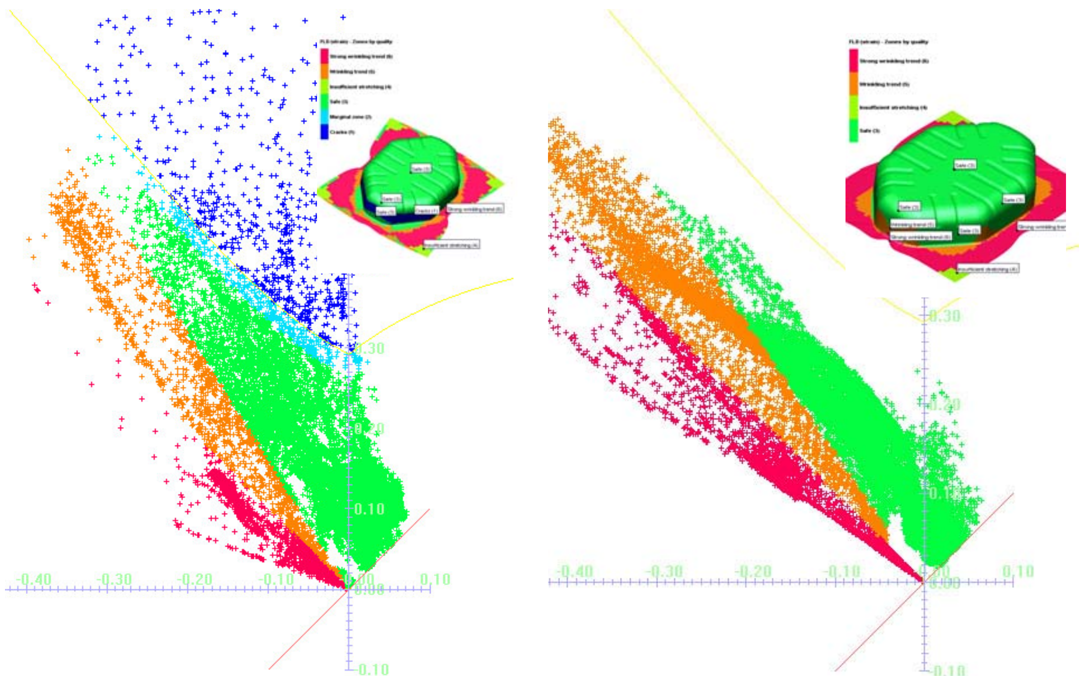

Figure 5.20: FLD variation with r_0

In figure 5.21 below, variation of FLD with r_{45} is shown. Apperently, r_{45} seems to affect the diagram lesser than the other coefficients, but this may not be a generalization because of the consideration of the interactions of many features that could influence the results to alter.

r_0 = 1.88 r_{45} = 0.5 r_{90} = 2.43 r_0 = 1.88 r_{45} = 2.5 r_{90} = 2.43

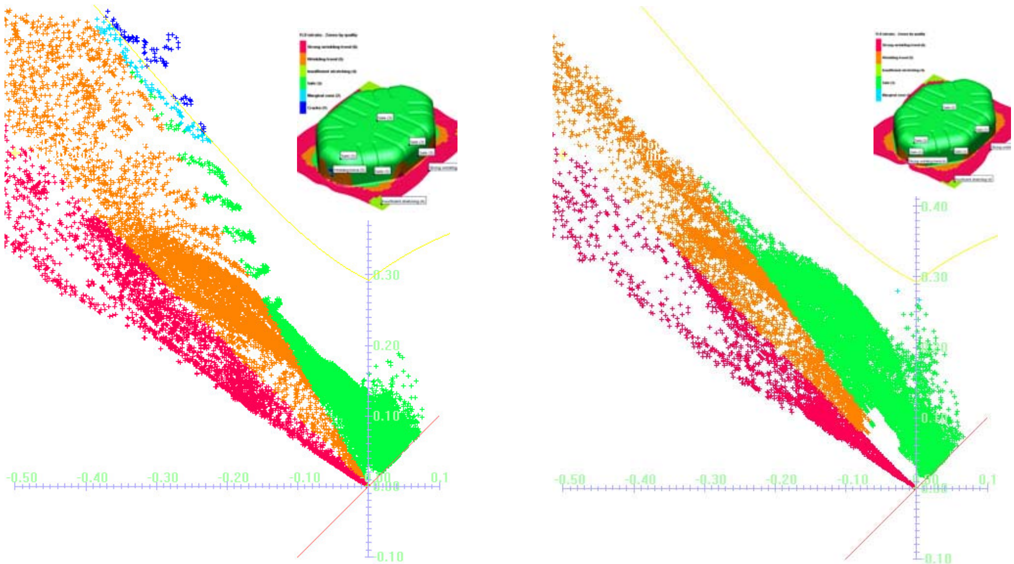

Figure 5.21: FLD variation with r_{45}

r_0 = 1.88 r_{45} = 1.87 r_{90} = 0.5 r_0 = 1.88 r_{45} = 1.87 r_{90} = 3

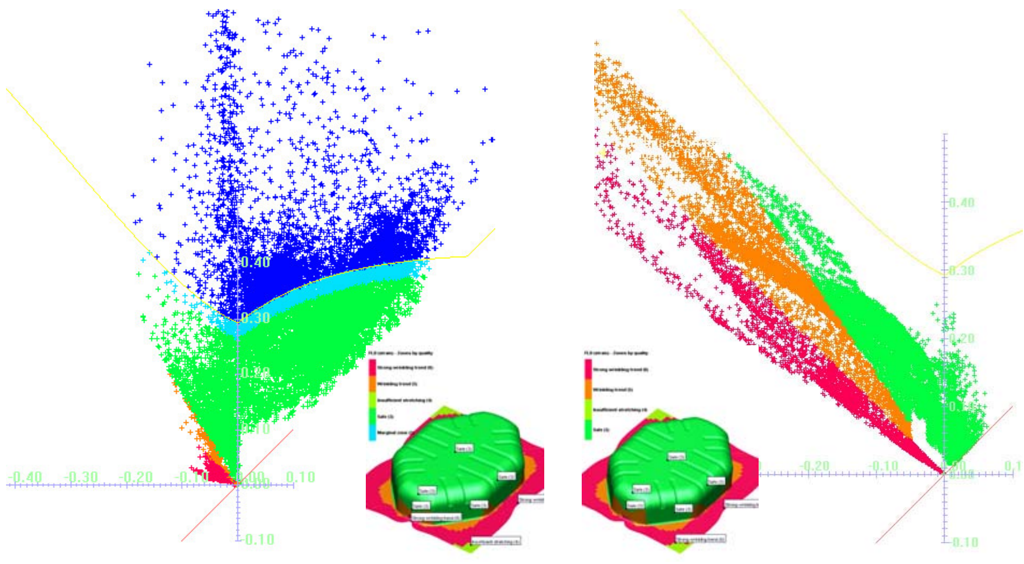

Figure 5.22: FLD variation with r_{90}

As it is seen from the simulation results of figures 5.5 - 5.22, variations among r values affect state of formability from different aspects. Zones of formability change respect to the change of r values, but variations are in different amounts. Also locations of points slide which are related with the same element .

Another comment from the results of analyses is the change of r_0 and r_{90} affect the results dramatically while change in r_{45} is not effective like others.

As a conclusion, calculation of r_0 and r_{90} must be made more carefully than the calculation of r_{45} for such kind of deep drawing processes.

5.5 Results of the drawing simulations comparing Hill 48, Hill 90 and Von Mises yield criteria

Before running analyses by using Hill 90 yield criterion, coefficients for this yield criterion must be calculated. Calculation of coefficients is possible by using material data in Pam-Stamp. For this reason, values of Table 5.3 was calculated in Pam Stamp. Von Mises Coefficients can be obtained by setting Lankford Coefficients to one [26, 31].

Table 5.3: Coefficients for Hill 90 Analysis

Coefficient	Value
α	2.27386
β	-0.376407
γ	-0.410404
m	2

As a conclusion, Hill 48 and Hill 90 coefficients were obtained by the means of uniaxial tensile test while further computation for Hill 90 values were made by Pam-Stamp software. In table 5.4 coefficients for other two yielding criteria are given.

Table 5.4: Coefficients for Hill 48 and Von Mises Analysis

Coefficient	Hill 48	Von Mises
r_0	1.88	1
r_{45}	1.87	1
r_{90}	2.43	1

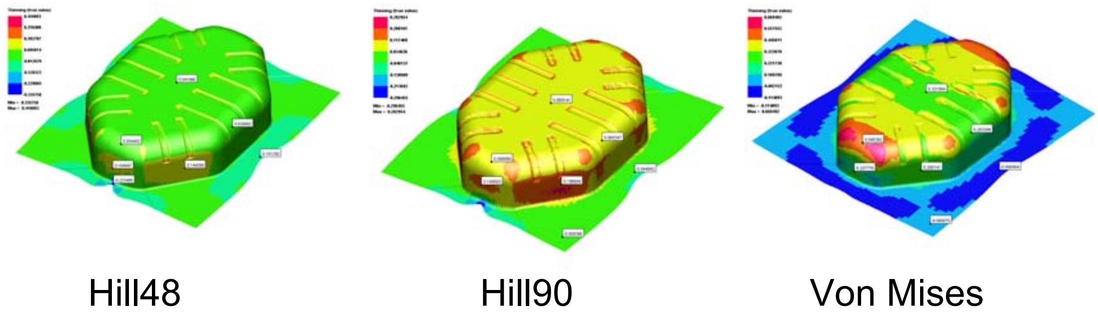

Figure 5.23: Thinning results of Hill 48, Hill 90 and Von mises

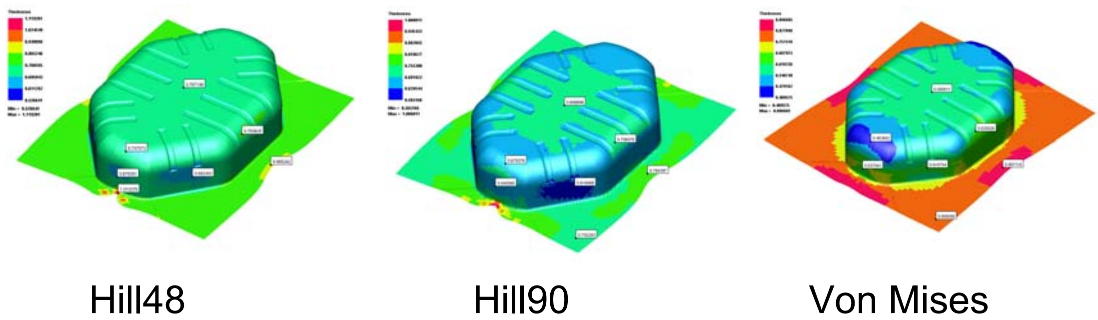

Figure 5.24: Thickness results of Hill 48, Hill 90 and Von mises

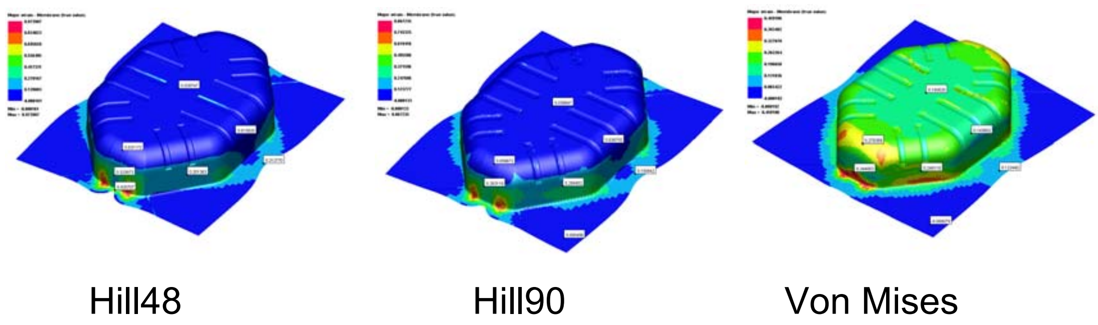

Figure 5.25: Major strain results of Hill 48, Hill 90 and Von mises

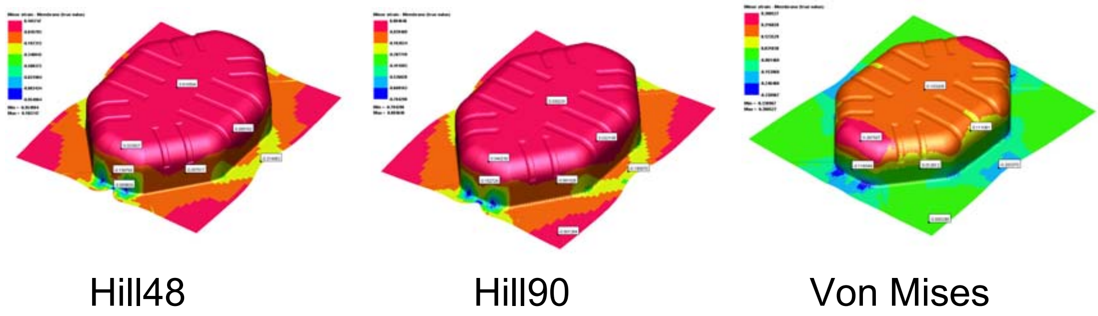

Figure 5.26: Minor strain results of Hill 48, Hill 90 and Von mises

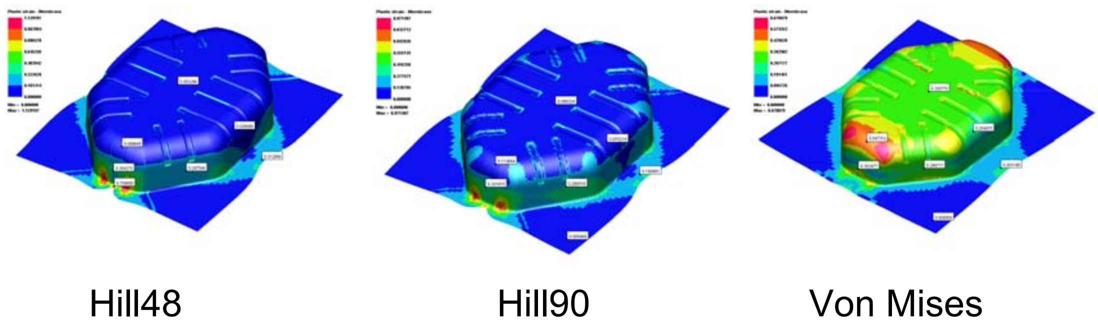

Figure 5.27: Plastic strain results of Hill 48, Hill 90 and Von mises

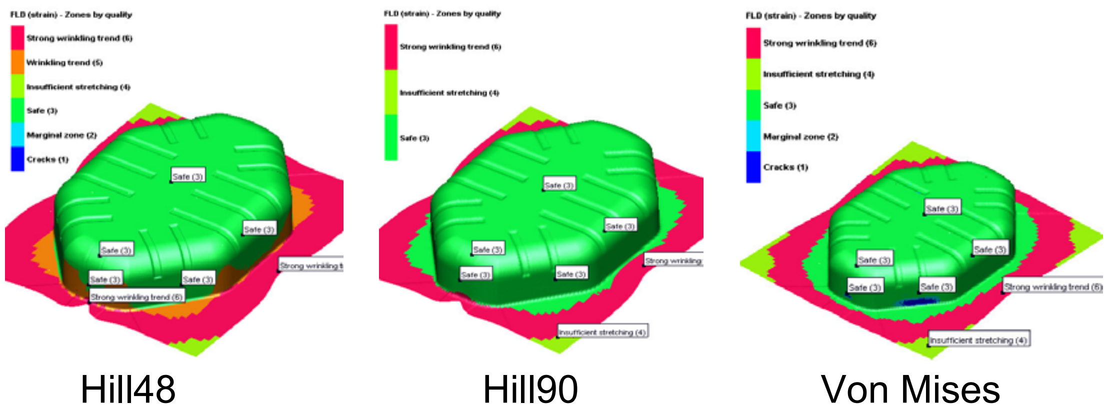

Figure 5.28: Results of formability zones of Hill 48, Hill 90 and Von mises

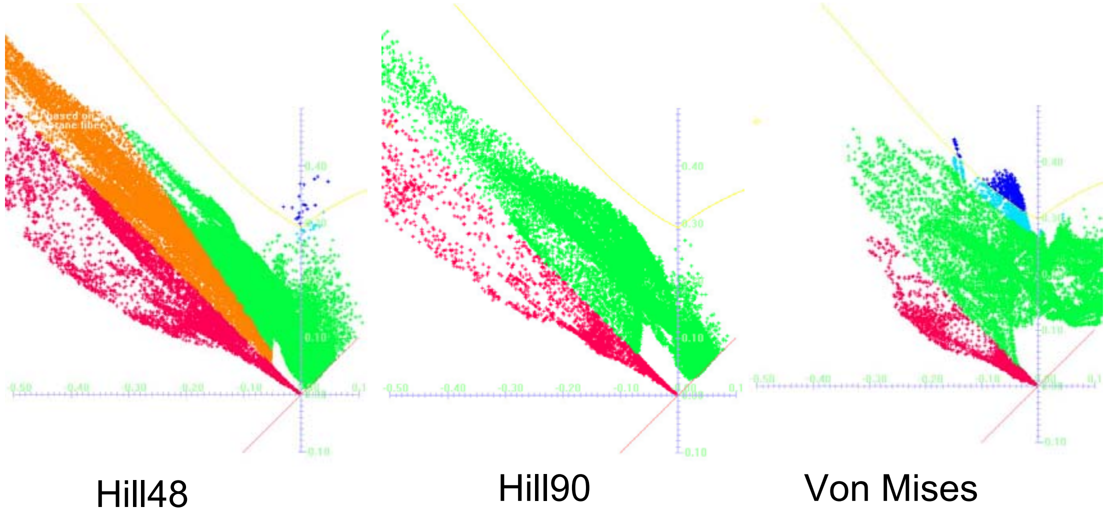

Figure 5.29: FLD results of Hill 48, Hill 90 and Von mises

According to the comparison of the simulation results and mesurements from the actual panel, Hill 48 is said to give more reliable results than the others. Regarding thinning and thickness measurements, values of the side wall and flange regions are so close to the simulation results. From the result of FLD diagram of Hill 48 solution, cracking regions are obtained which are can be seen in the thinning or thickness simulations also. Moreover, these results fit to the measurements of the actual panel. Another important point is the wrinkling results. In Hill 48 simulations, there are regions that have wrinkling tendency while in Hill 90 simulations there are no regions that have wrinkling tendency observed.

Although the calculations are not accurate in this work, Hill 90 solutions are expected to be more accurate than the Hill 48 solutions according to the papers related to this field . Probable mistake may be the miscalculated coefficients for this yield criteria.

As it is seen from the results of the Von Mises solution, thinning, thickness and the shape of the panel of simulations are not even close to the real data. From these results, one can understand the significance of using anisotropic yield criteria while working with the sheet metals.

5.6 Results of the contact force and punch penetration comparing Hill 48 Hill 90 and Von Mises yielding criteria

According to the contact force vs. punch penetration results, it is obtained that punch penetrates about 185 mm. which is also nearly the height of the wheelhouse panel and at the and of this penetration, punch force yields about 600 kN. In the simulation applications, BHF is adjusted to obtain the panel without any wrinkles or cracks and which is later to be added to the punch force to obtain the minimum press tonnage.

In the simulation results non of these three yield criteria make any difference until the end of the penetration process. The peak after 185 mm is related to the contact of the punch, die and sheet interaction.

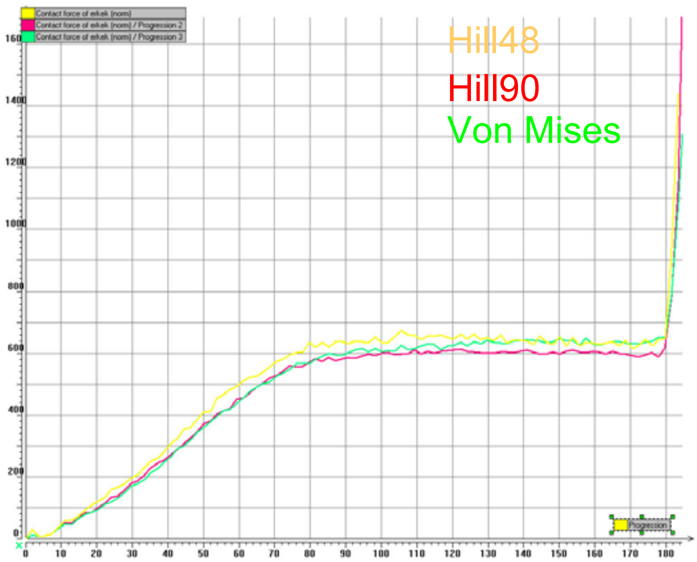

Figure 5.30: Contact force results of Hill 48, Hill 90 and Von Mises

In figure 5.31 strain path forming for different Lankford Coefficients are obtained. According to this figure, different Lankford Coefficients create different strain paths. So, it is one of the ways to explain the strain path orientation in FLD diagrams for the same element with same material under different Lankford Coefficients.

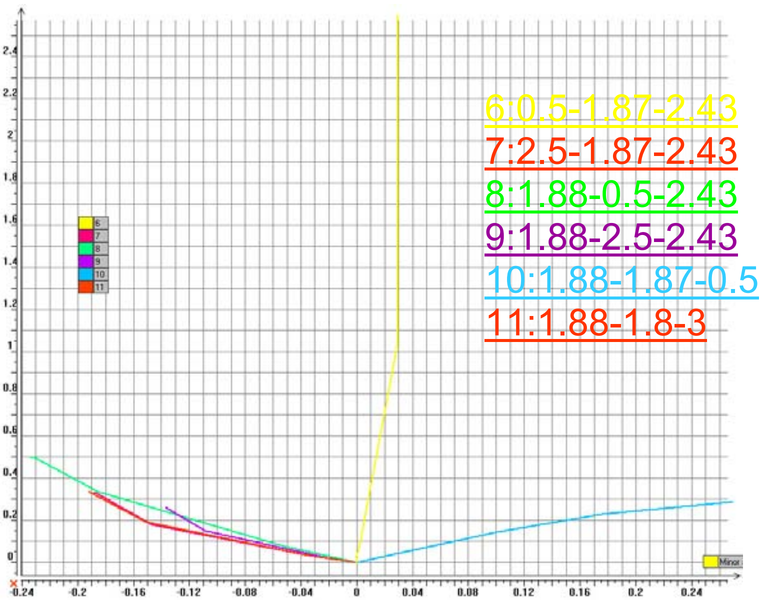

Figure 5.31: Strain paths for different anisotropy coefficients

5.7 Comparison of the results by using normal anisotropy value of 2.01 and Lankford Coefficients of 1.88, 1.87 and 2.43

As it is mentioned before calculation of the normal anisotropy value can be made according to the equation (4.2). According to this equation, normal anisotropy value for the used material is 2.01. This section is separated from 5.8 because the material data and Lankford Coefficients which are used in this section are taken from the test results.

Results of analyses of these two cases are below:

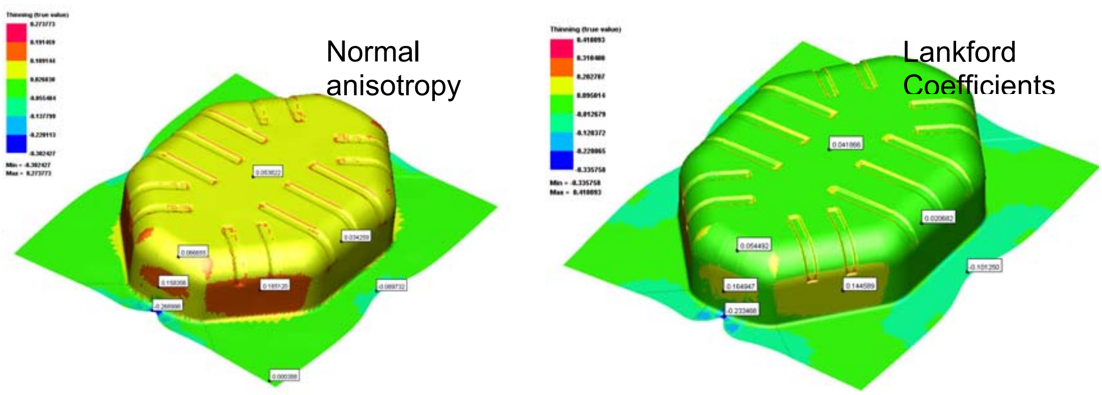

Figure 5.32: Thinning results with r values of 1.88, 1.87, 2.43 and R of 2.01

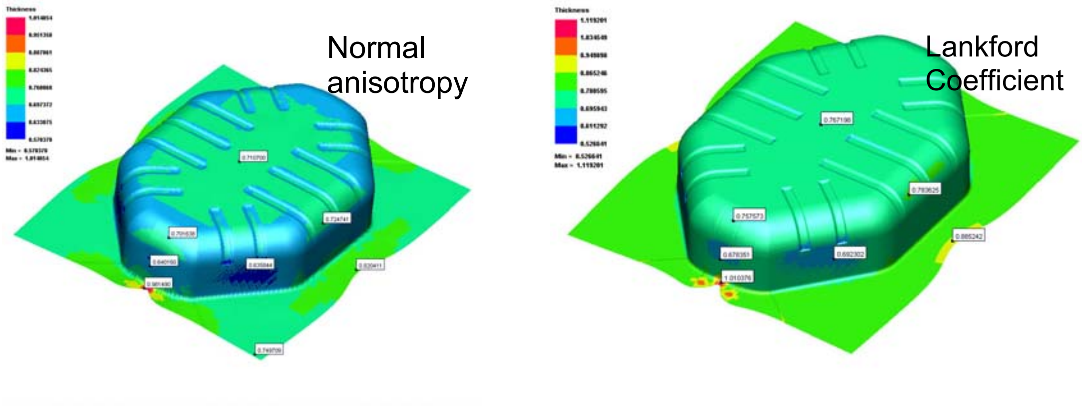

Figure 5.33: Thickness results with r values of 1.88, 1.87, 2.43 and R of 2.01

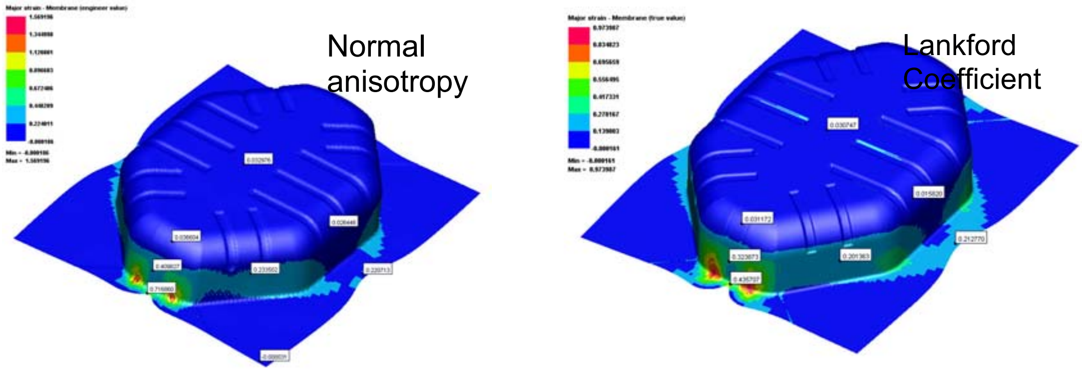

Figure 5.34: Major strain results with r values of 1.88, 1.87, 2.43 and R of 2.01

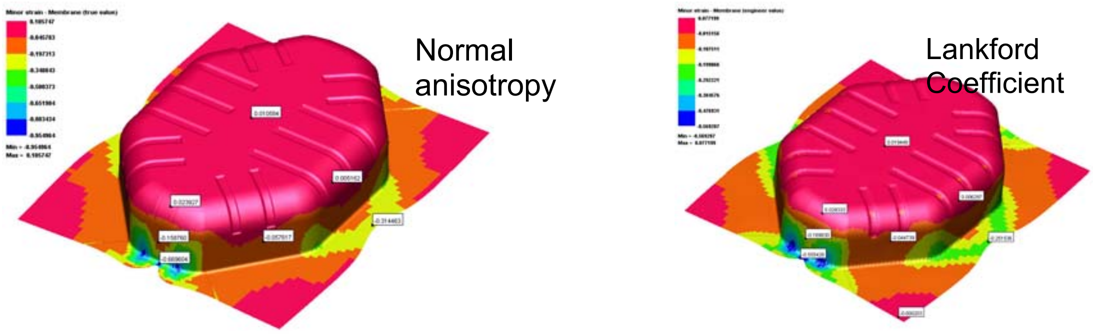

Figure 5.35: Minor strain results with r values of 1.88, 1.87, 2.43 and R of 2.01

Although the values of Lankford Coefficients are not far apart from 2.01, all results have variations when they are compared. By the way, results of both analyses can be compared with the actual panel data to figure out which method yield better results.

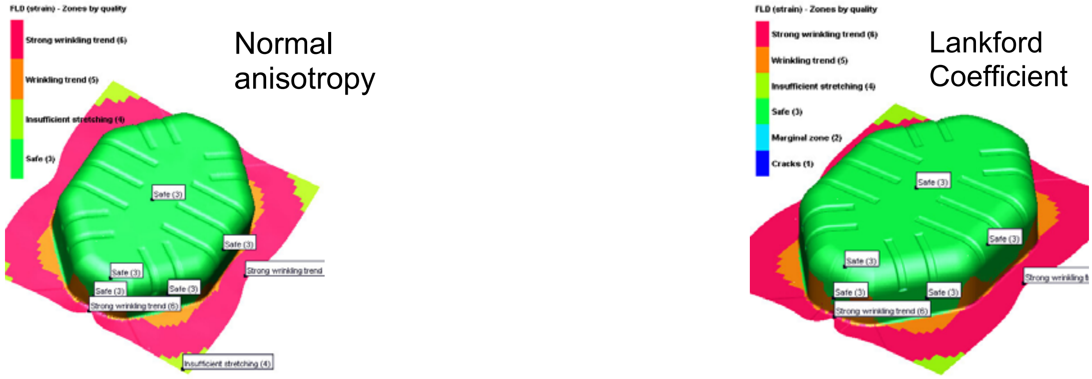

Figure 5.36: Formability zone results with r values of 1.88, 1.87, 2.43 and R of 2.01

Figure 5.37: FLD results with r values of 1.88, 1.87, 2.43 and R of 2.01

According to the figures 5.32 - 5.37, results of the same points are varying and results that are obtained with the Lankford coefficients are more reliable than the results obtained with normal anisotropy value according to the measures of actual panel. Actual panel fails near flange and side wall curl regions as it seen from the simulation results that are performed by Lankford coefficients.

5.8 Comparison of the simulation results by using Lankford Coefficients that have normal anisotropy value of 2.01

The aim of this examination is to show the differences in the results of different Lankford Coefficients that yield the value of 2.01 as the normal anisotropy coefficient when put in the equation (4.2). By this application, variations among the results of Lankford Coefficient's and normal anisotropy can be figured out. Additionally, since these coefficients are not as same as the measured coefficients or actual material data, results are not compared with the actual panel. On the other hand, the goal of this section is to find an answer to the question of using normal anisotropy value in simulations The coefficients subjected to this study can be seen in the table 5.5 below.

Table 5.5: Lankford Coefficients which were set to obtain normal anisotropy value of 2.01

Analysis	r0	r45	r90	R
1	2.43	1.88	1.87	2.01
2	1.88	2.15	1.87	2.01
3	2.35	1.7	2.3	2.01
4	2.1	1.9	2.15	2.01
5	1.8	2.1	2.05	2.01
6	1	2.28	2.5	2.01
7	2.92	1.1	2.92	2.01
8	2.5	2.28	1	2.01

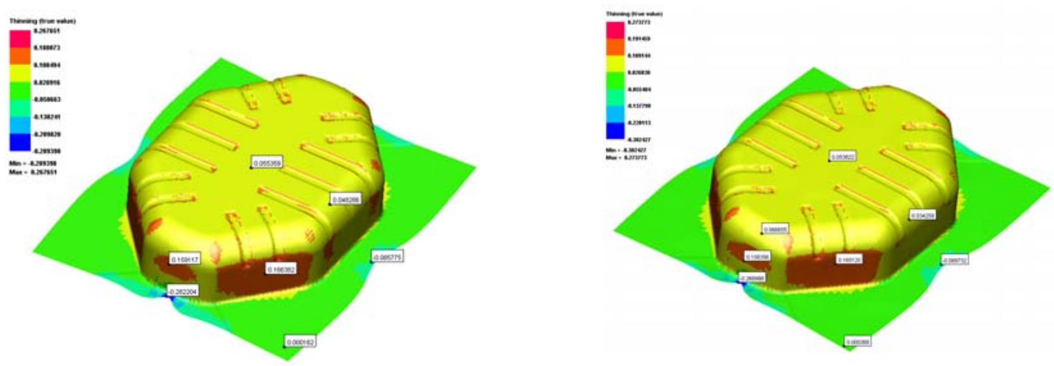

Figure 5.38: Thinning results with r values of 2.43, 1.88, 1.87 and R value of 2.01

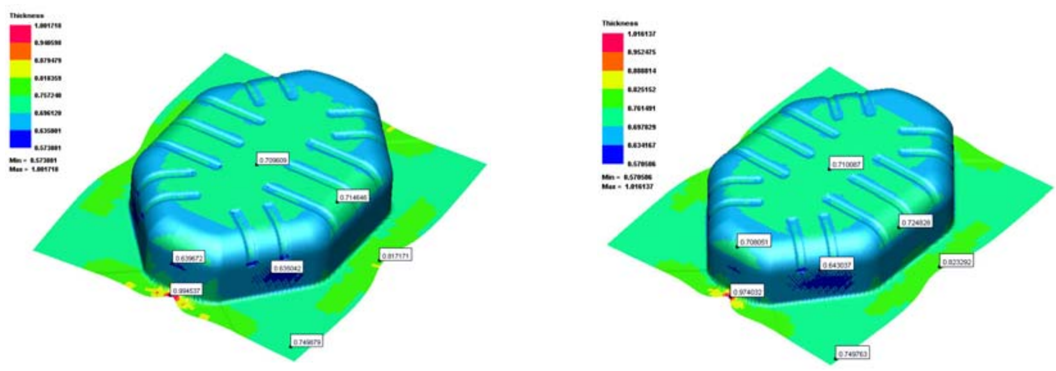

Figure 5.39: Thickness results with r values of 2.43, 1.88, 1.87 and R value of 2.01

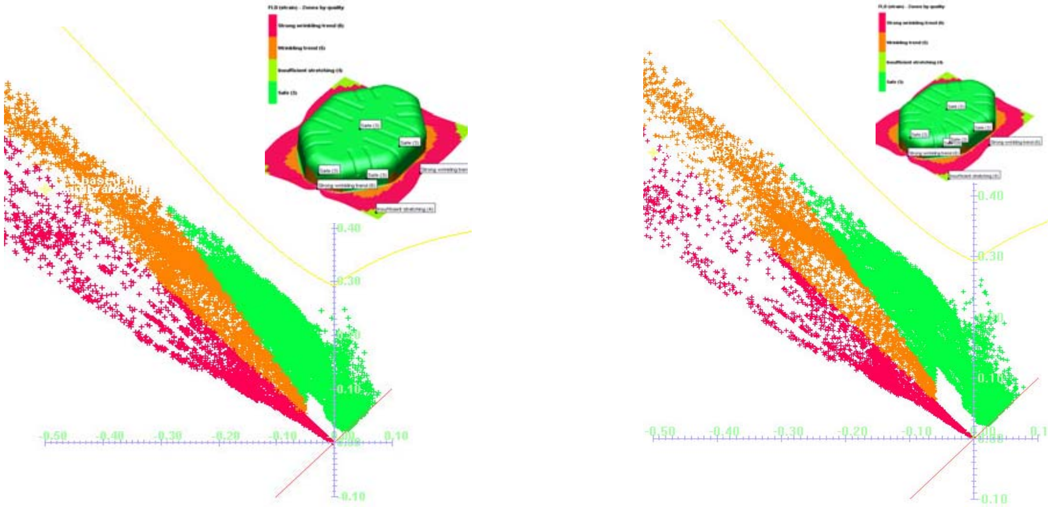

Figure 5.40: FLD results with r values of 2.43, 1.88, 1.87 and R value of 2.01

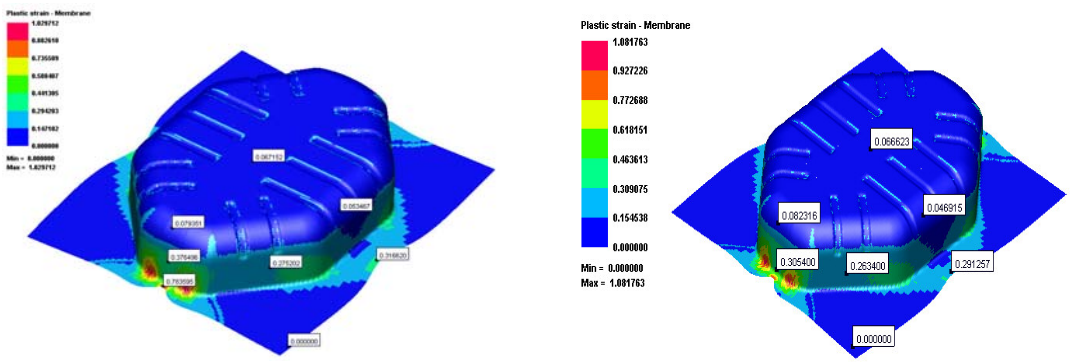

Figure 5.41: Plastic strain results with r values of 2.43, 1.88, 1.87 and R value of 2.01

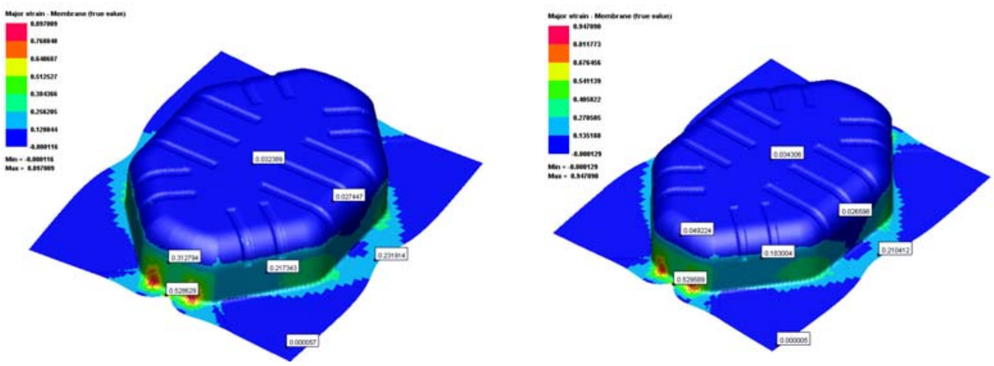

Figure 5.42: Major strain results with r values of 2.43, 1.88, 1.87 and R value of 2.01

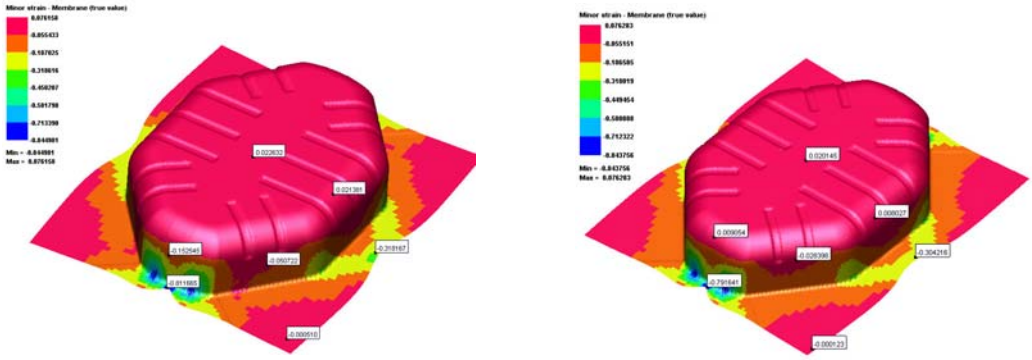

Figure 5.43: Minor strain results with r values of 2.43, 1.88, 1.87 and R value of 2.01

As a result for this simulations according to the figures 5.38 - 5.43, results at the same points are not change significantly. Results of the FLD are not change either. At a glance, results seem to be very close but one must bear in mind that, the order of anisotropy values were altered.

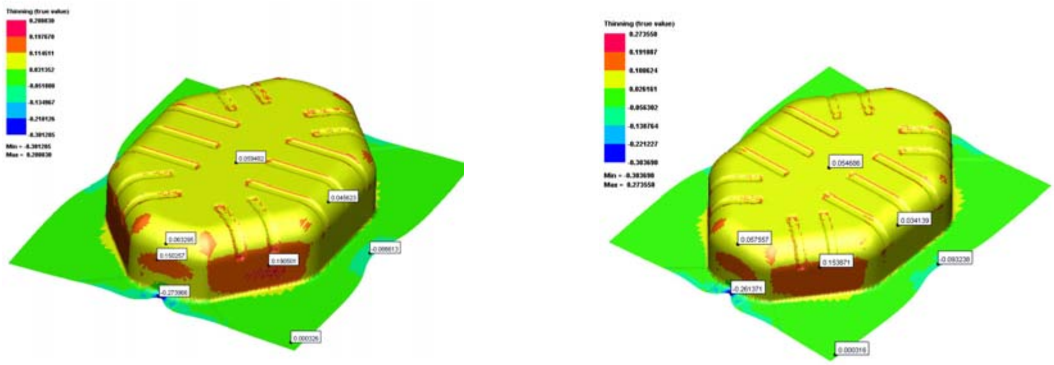

Figure 5.44: Thinning results with r values of 1.88, 2.15, 1.87 and R value of 2.01

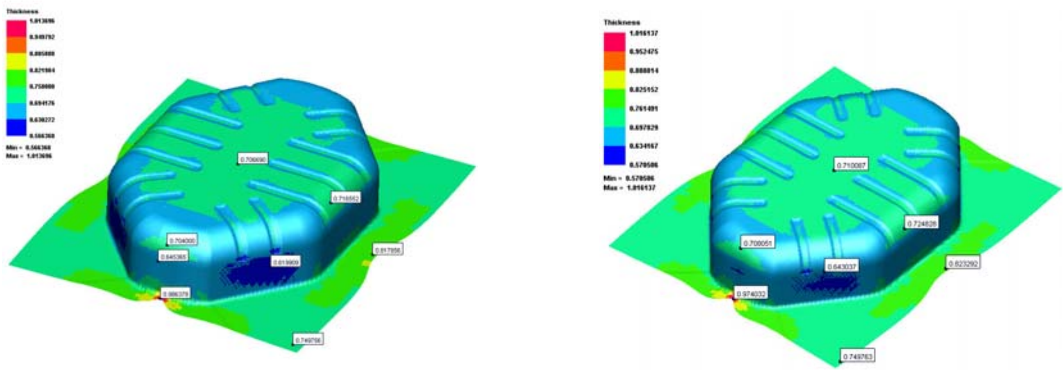

Figure 5.45: Thickness results with r values of 1.88, 2.15, 1.87 and R value of 2.01

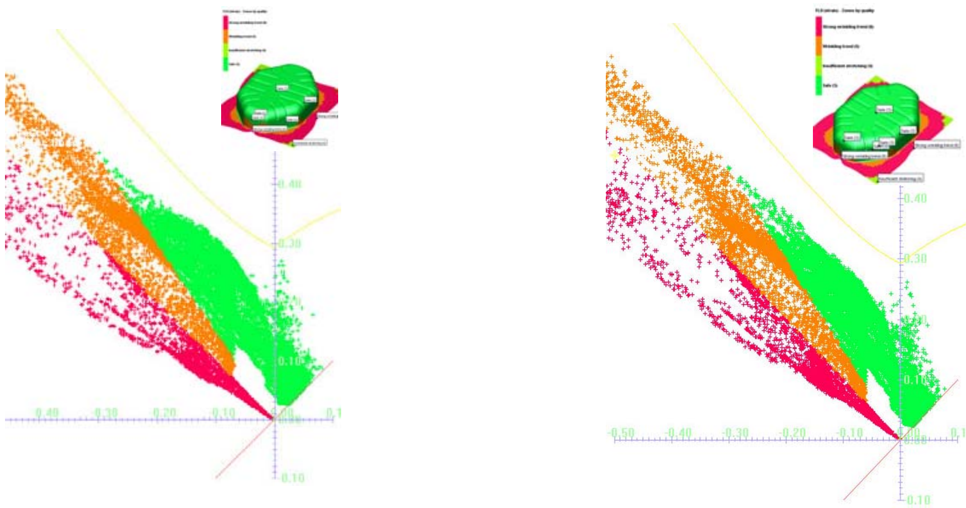

Figure 5.46: FLD results with r values of 1.88, 2.15, 1.87 and R value of 2.01

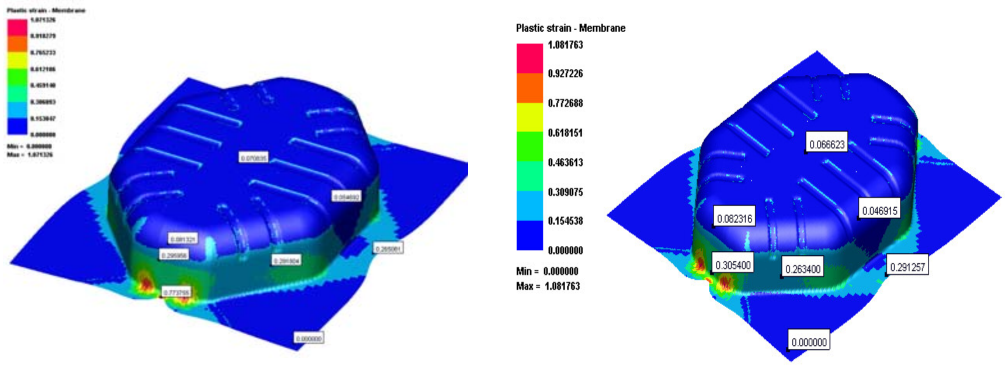

Figure 5.47: Plastic strain results with r values of 1.88, 2.15, 1.87 and R value of 2.01

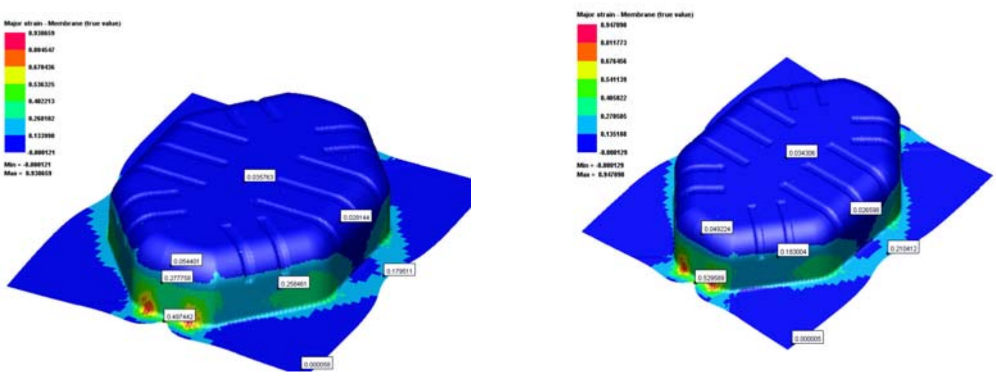

Figure 5.48: Major strain results with r values of 1.88, 2.15, 1.87 and R value of 2.01

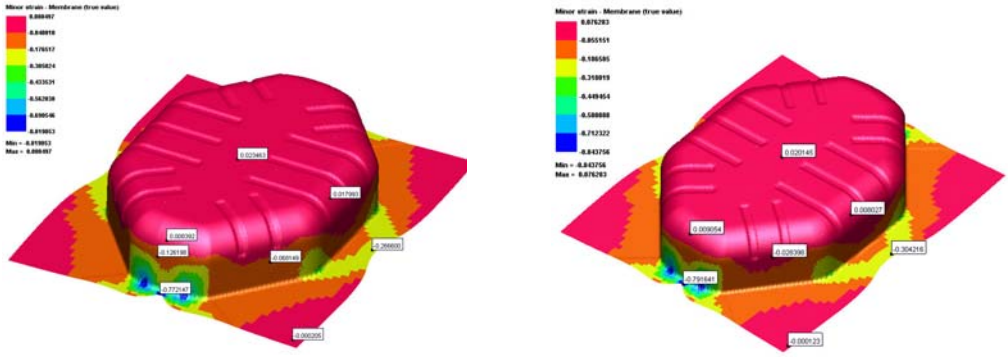

Figure 5.49: Minor strain results with r values of 1.88, 2.15, 1.87 and R value of 2.01

According to the figures 5.44 - 5.49, results of the same points of regions are changing. The variations are especially in the flange and side wall regions but, they are not significant to be considered. Also FLD results of the simulations are nearly same.

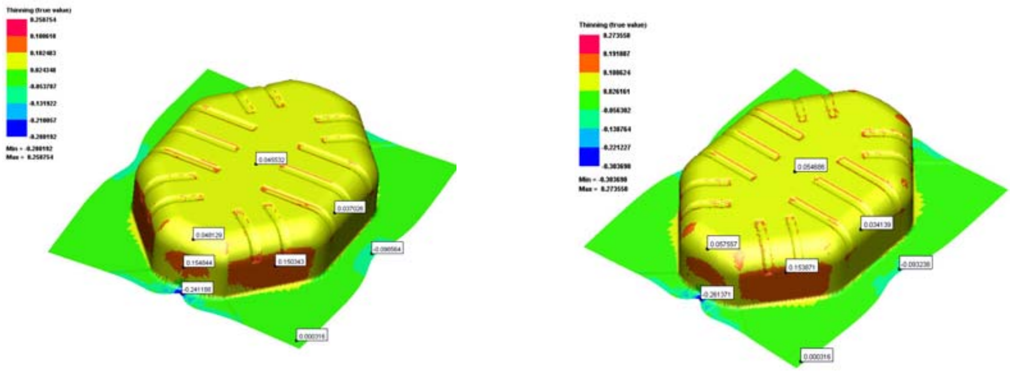

Figure 5.50: Thinning results with r values of 2.35, 1.7, 2.3 and R value of 2.01

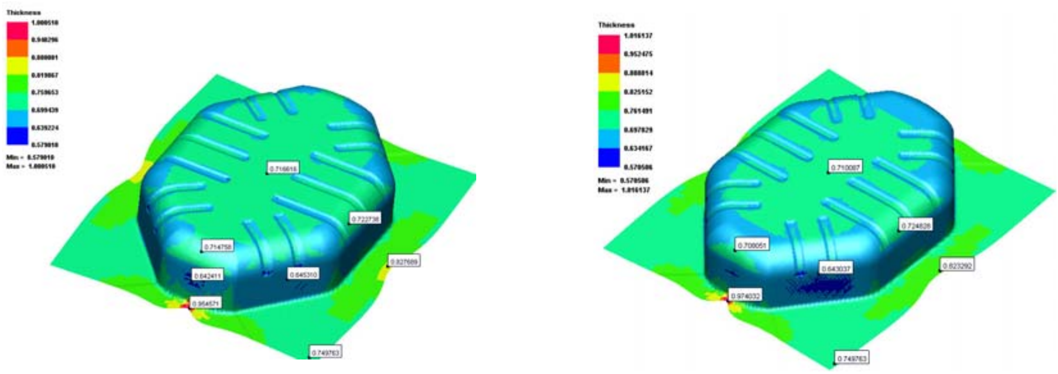

Figure 5.51: Thickness results with r values of 2.35, 1.7, 2.3 and R value of 2.01

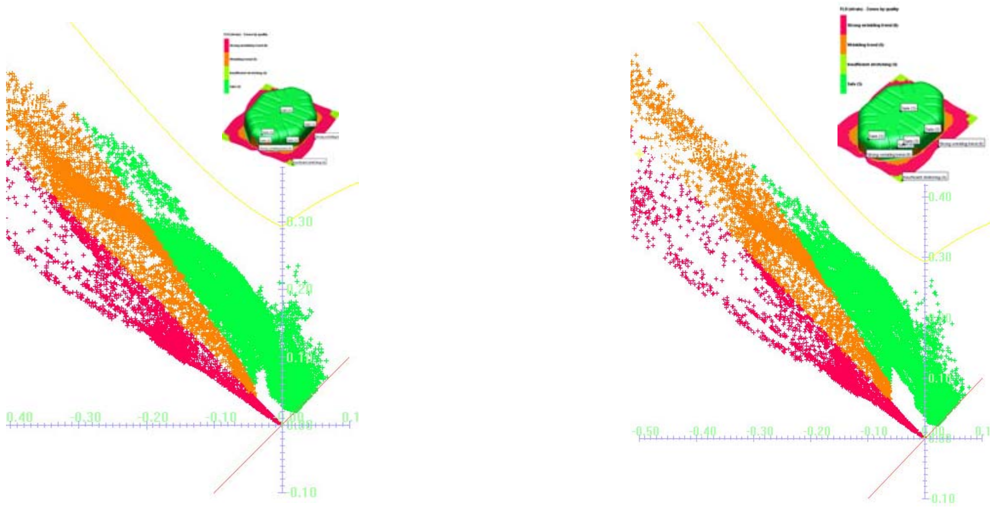

Figure 5.52: FLD results with r values of 2.35, 1.7, 2.3 and R value of 2.01

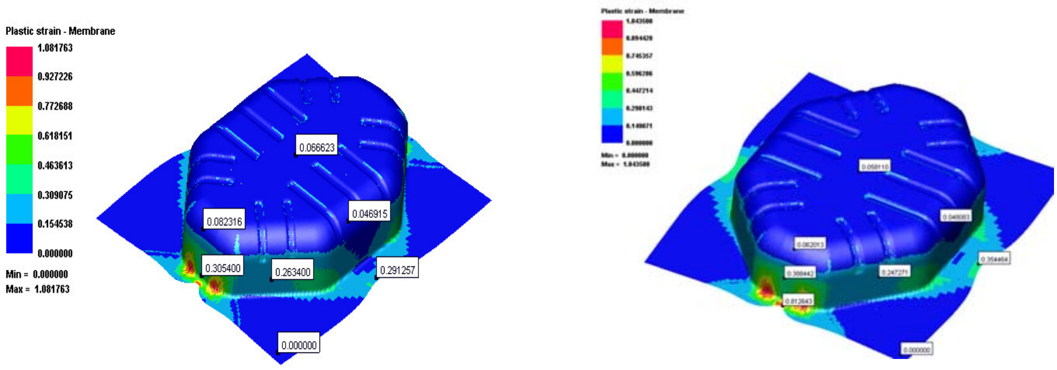

Figure 5.53: Plastic strain results with r values of 2.35, 1.7, 2.3 and R value of 2.01

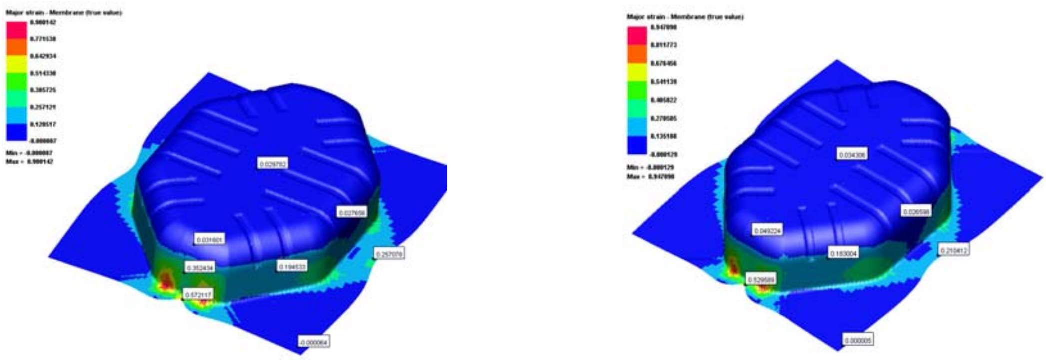

Figure 5.54: Major strain results with r values of 2.35, 1.7, 2.3 and R value of 2.01

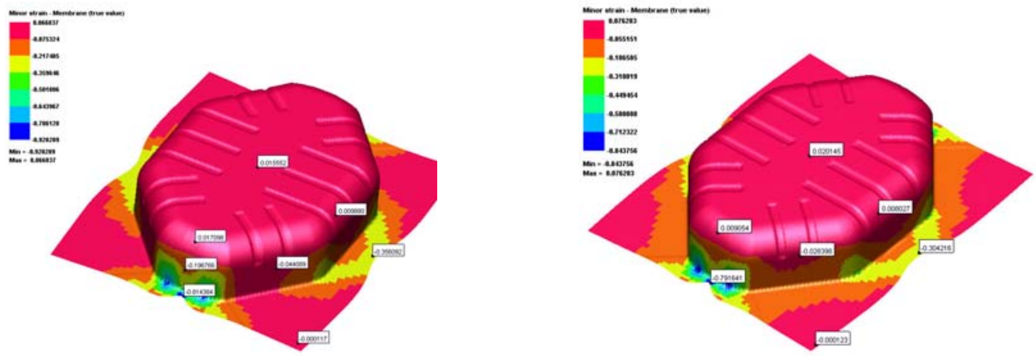

Figure 5.55: Minor strain results with r values of 2.35, 1.7, 2.3 and R value of 2.01

According to the figures 5.50- 5.55, results of the same points are not change significantly. Beside this, FLD is not indicate any major variation.

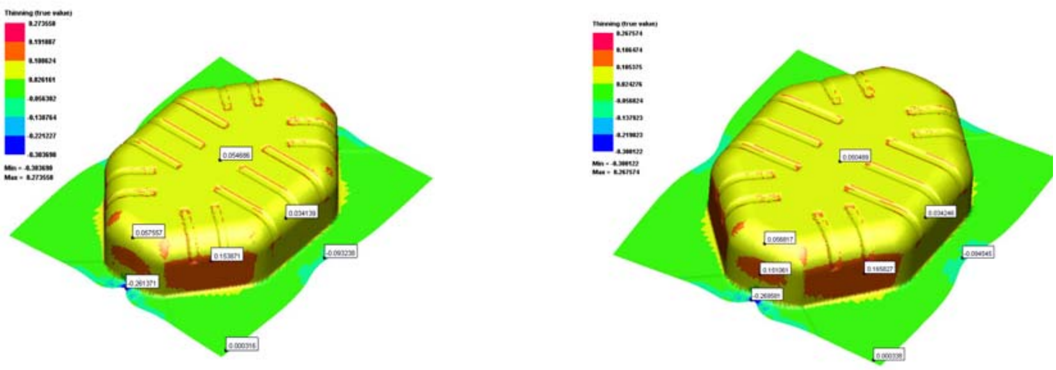

Figure 5.56: Thinning results with r values of 2.1, 1.9, 2.15 and R value of 2.01

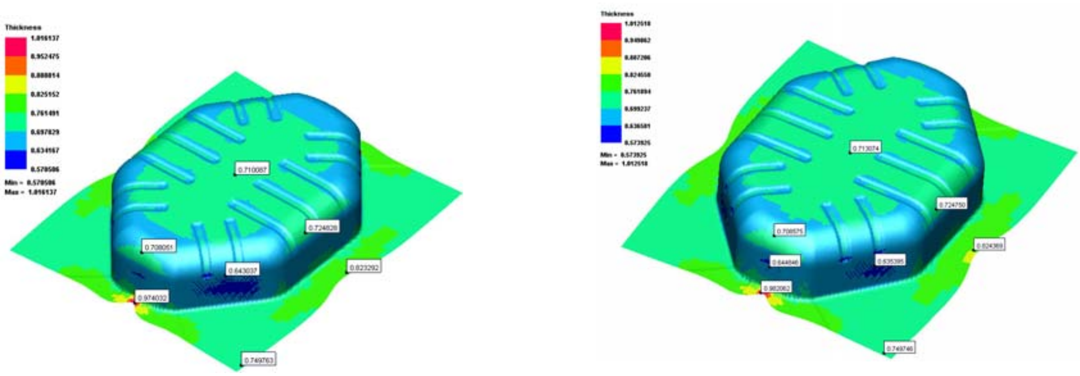

Figure 5.57: Thickness results with r values of 2.1, 1.9, 2.15 and R value of 2.01

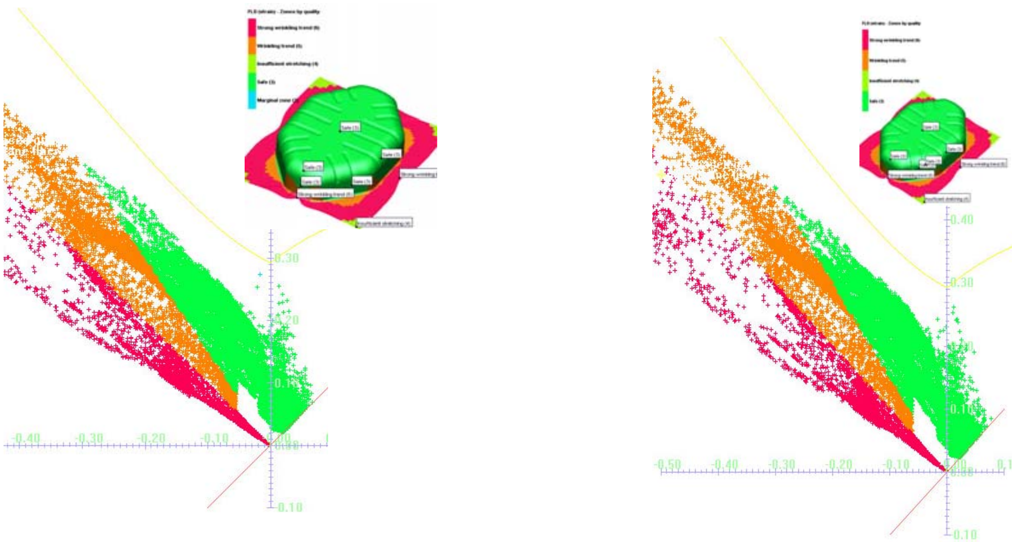

Figure 5.58: FLD results with r values of 2.1, 1.9, 2.15 and R value of 2.01

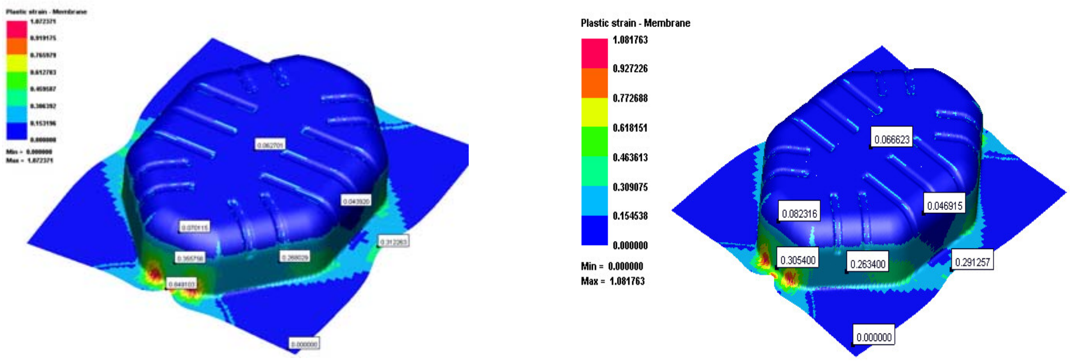

Figure 5.59: Plastic strain results with r values of 2.1, 1.9, 2.15 and R value of 2.01

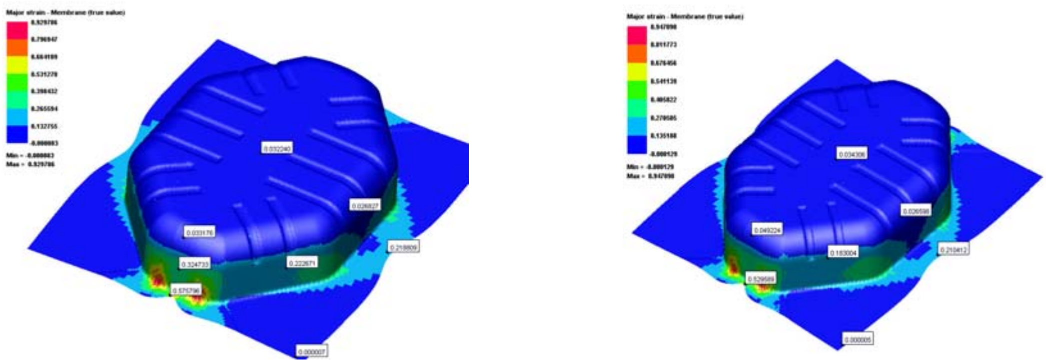

Figure 5.60: Major strain results with r values of 2.1, 1.9, 2.15 and R value of 2.01

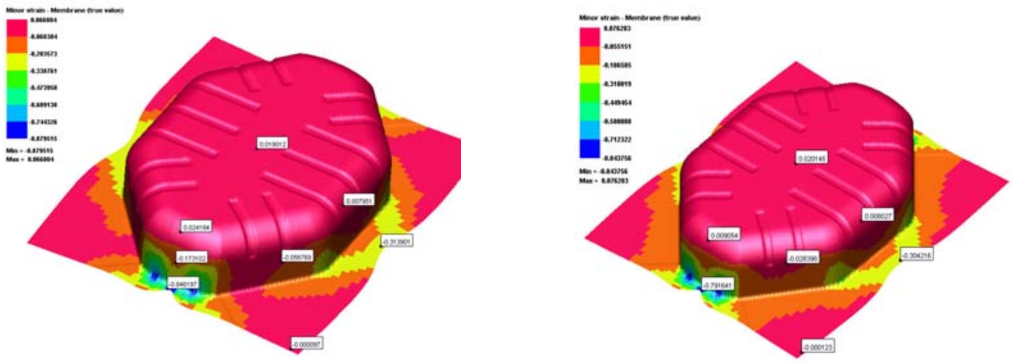

Figure 5.61: Minor strain results with r values of 2.1, 1.9, 2.15 and R value of 2.01

According to the figures 5.56 - 5.61, results at the same points are close to each other but, as it is seen, marginal zone result is obtained which could fail the panel due to different Lankford Coefficients and it is not seen in the normal anisotropy results.

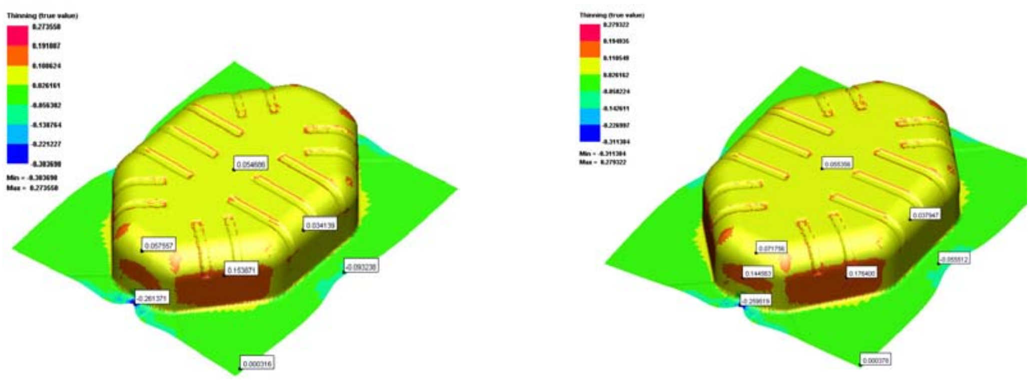

Figure 5.62: Thinning results with r values of 1.8, 2.1, 2.05 R value of 2.01

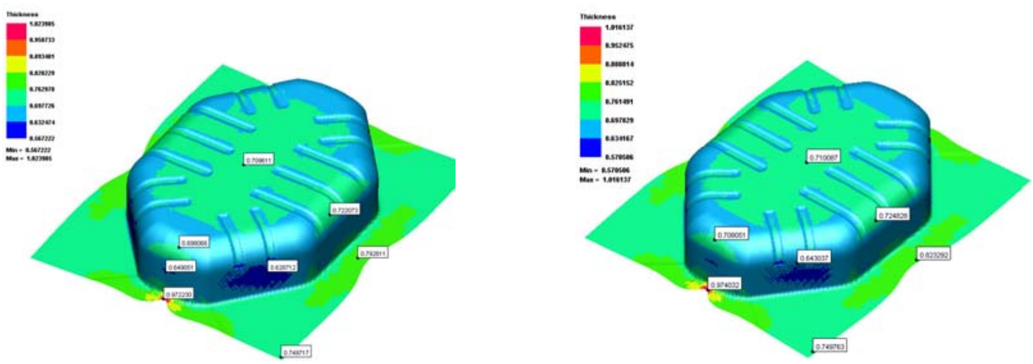

Figure 5.63: Thickness results with r values of 1.8, 2.1, 2.05 and R value of 2.01

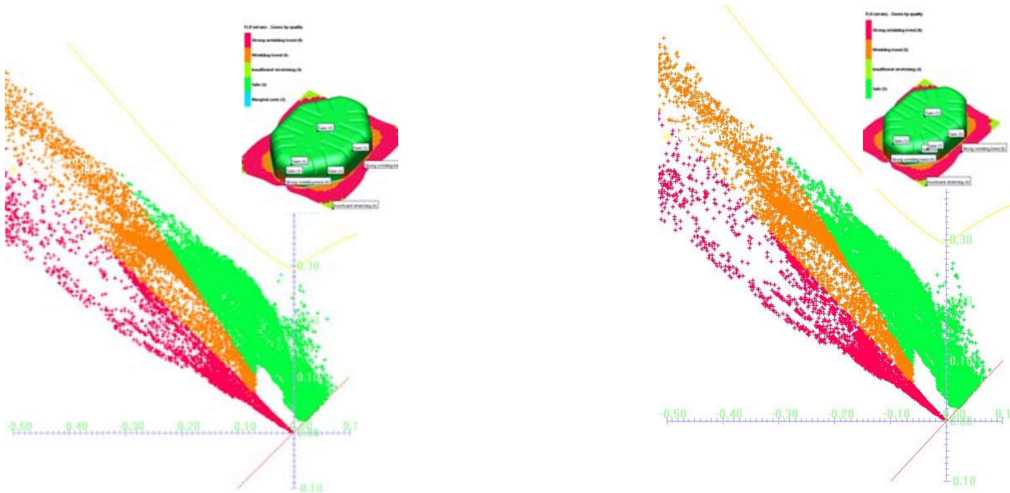

Figure 5.64: FLD results with r values of 1.8, 2.1, 2.05 and R value of 2.01

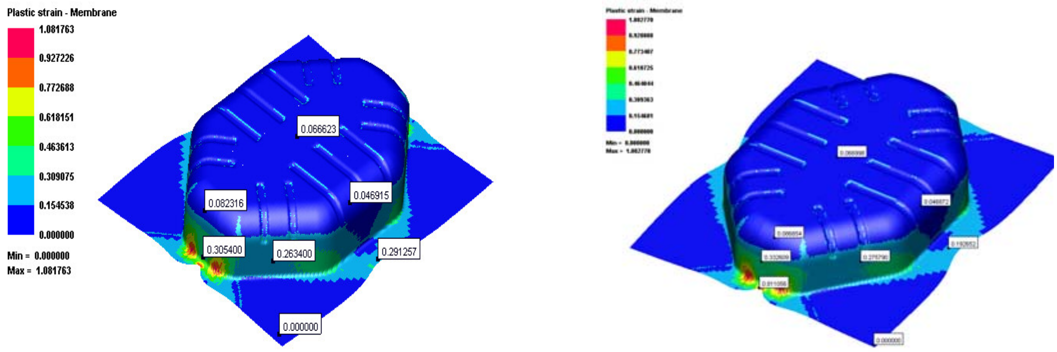

Figure 5.65: Plastic strain results with r values of 1.8, 2.1, 2.05 and R value of 2.01

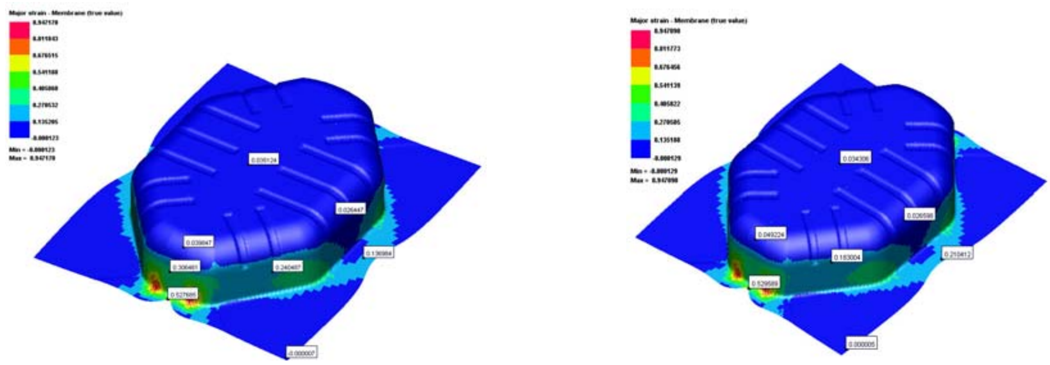

Figure 5.66: Major strain results with r values of 1.8, 2.1, 2.05 and R value of 2.01

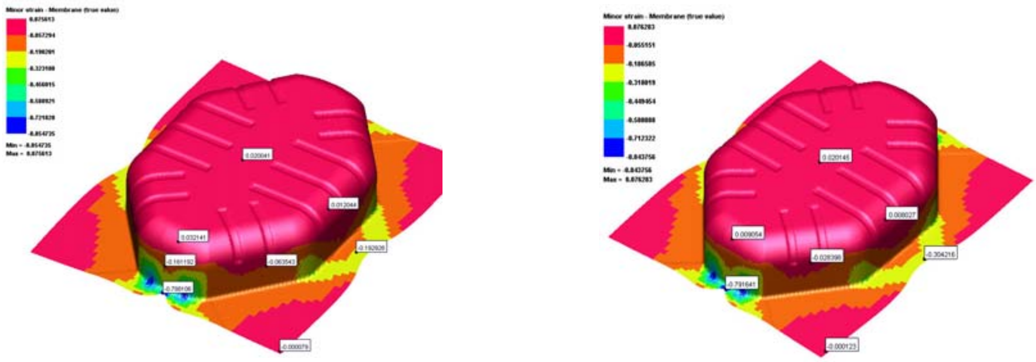

Figure 5.67: Minor strain results with r values of 1.8, 2.1, 2.05 and R value of 2.01

According to the figures 5.62- 5.67, some results of the same points are not changed significantly but, for some points, marginal zone result is obtained which could fail the panel due to different Lankford Coefficients.

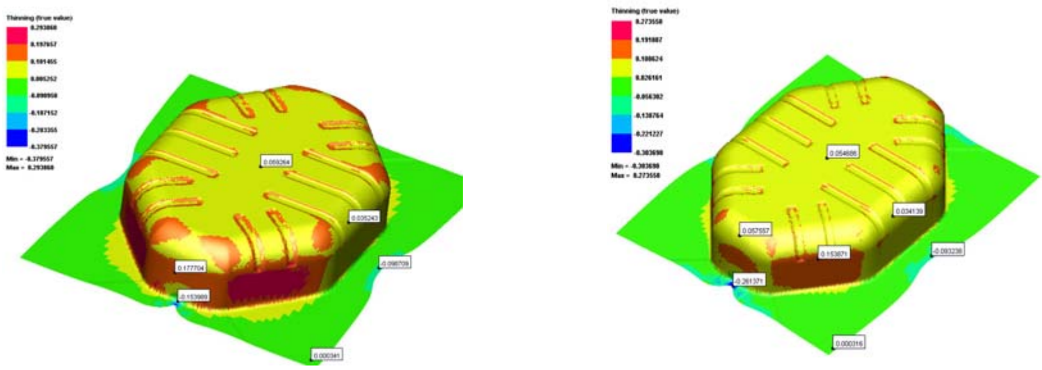

Figure 5.68: Thinning results with r values of 1, 2.28, 2.5 and R value of 2.01

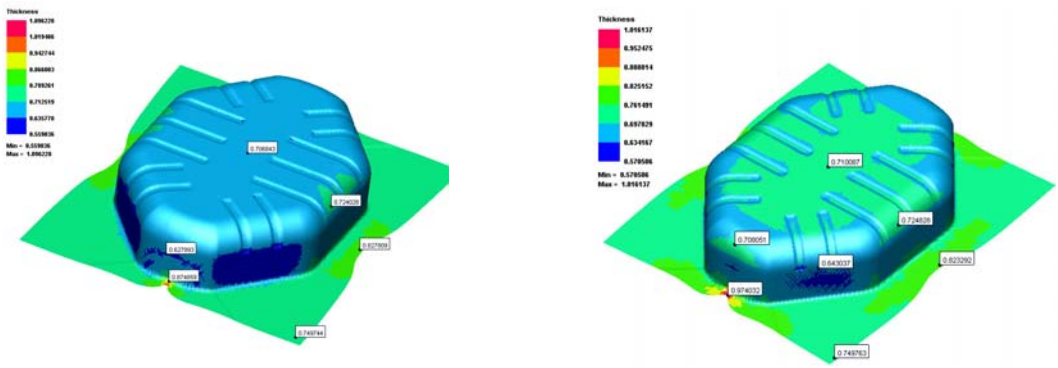

Figure 5.69: Thickness results with r values of 1, 2.28, 2.5 and R value of 2.01

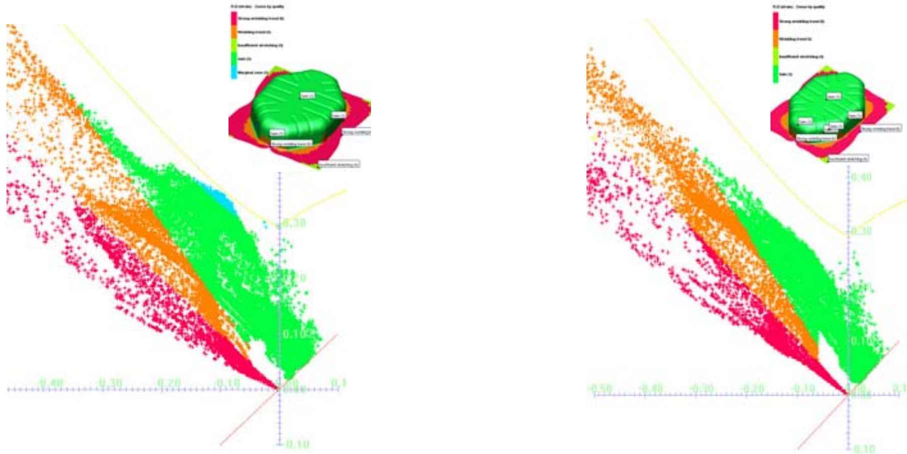

Figure 5.70: FLD results with r values of 1, 2.28, 2.5 and R value of 2.01

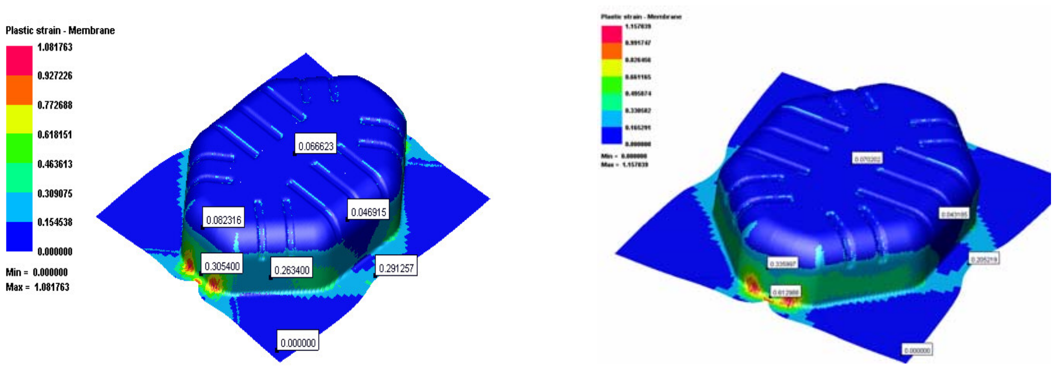

Figure 5.71: Plastic strain results with r values of 1, 2.28, 2.5 and R value of 2.01

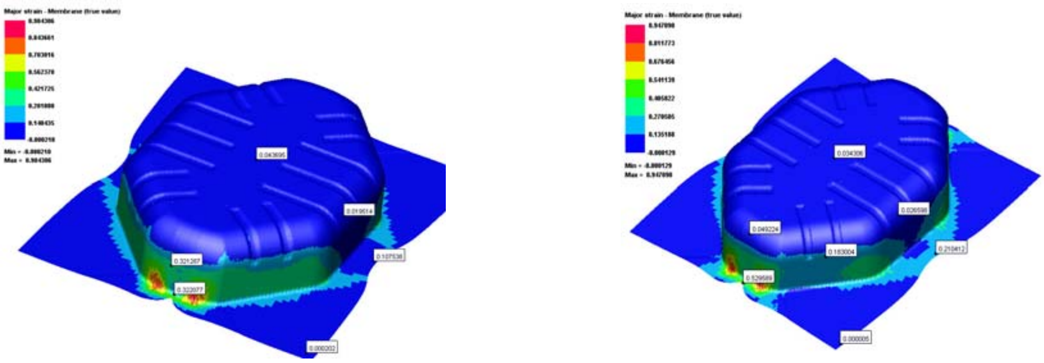

Figure 5.72: Major Strain results with r values of 1, 2.28, 2.5 and R value of 2.01

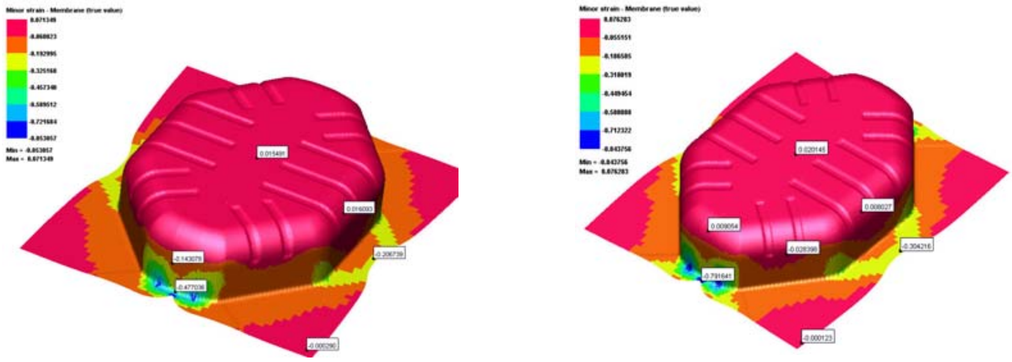

Figure 5.73: Minor strain results with r values of 1, 2.28, 2.5 and R value of 2.01

According to the figures 5.68 - 5.73, overall thinning or thickness are not change significantly except flange and side wall regions. On the other hand, many points prone to enter the cracking zone according to the FLD, which is not seen with normal anisotropy solution. Also, variation of r_0 must be taken into consideration for this results.

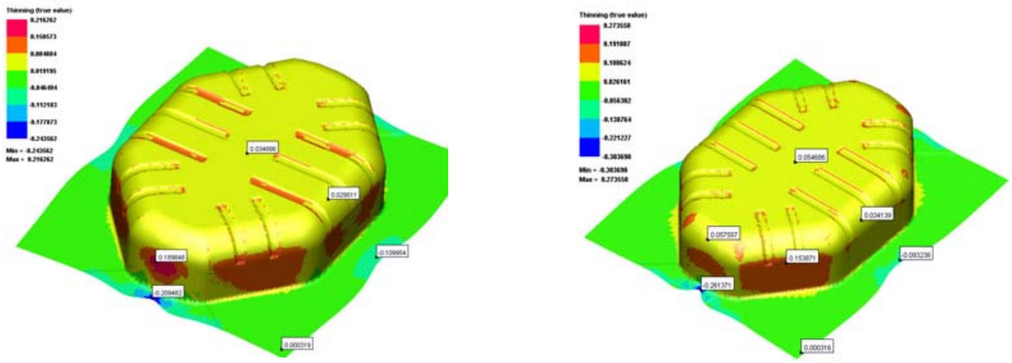

Figure 5.74: Thinning results with r values of 2.92, 1.1, 2.92 and R value of 2.01

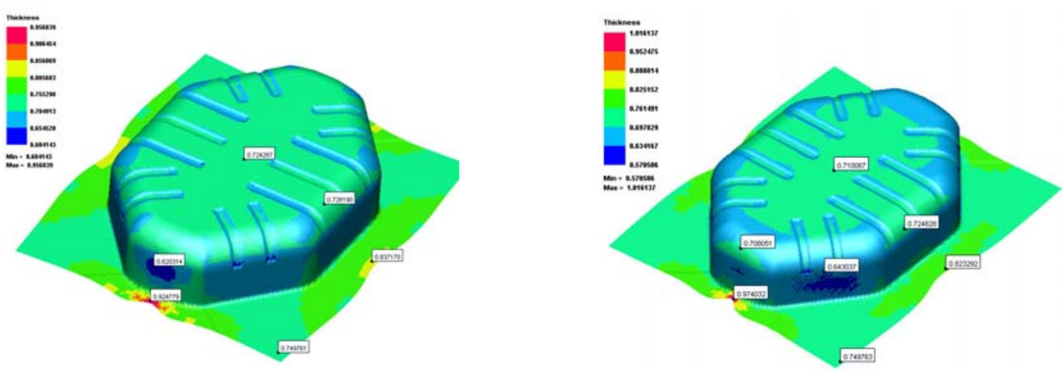

Figure 5.75: Thickness results with r values of 2.92, 1.1, 2.92 and R value of 2.01

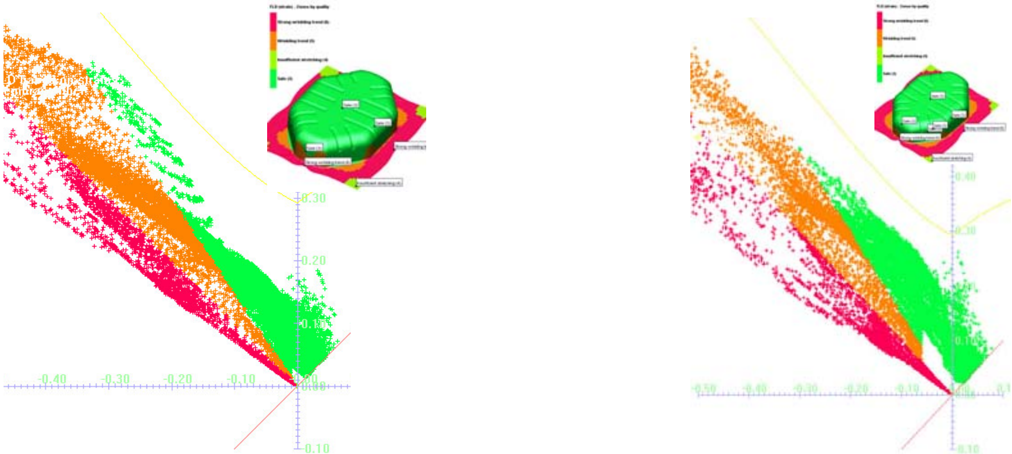

Figure 5.76: FLD results with r values of 2.92, 1.1, 2.92 and R value of 2.01

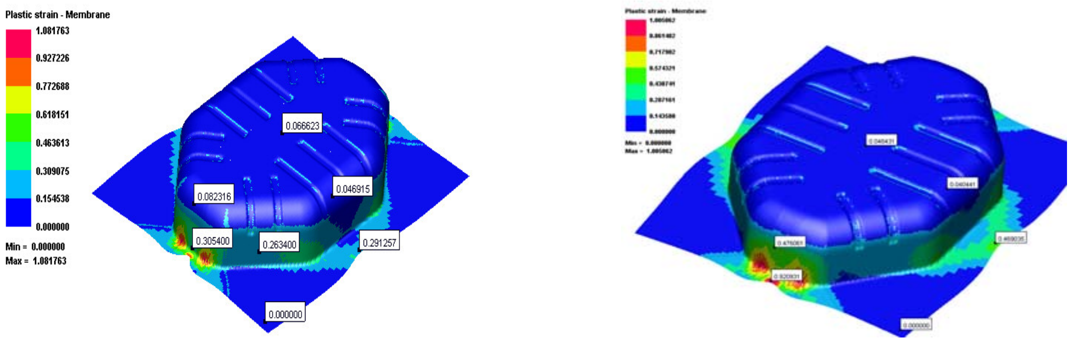

Figure 5.77: Plastic strain results with r values of 2.92, 1.1, 2.92 and R value of 2.01

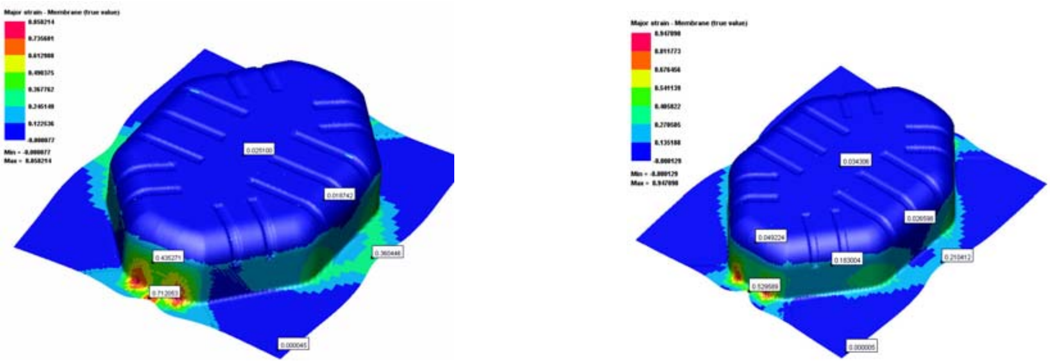

Figure 5.78: Major strain results with r values of 2.92, 1.1, 2.92 and R value of 2.01

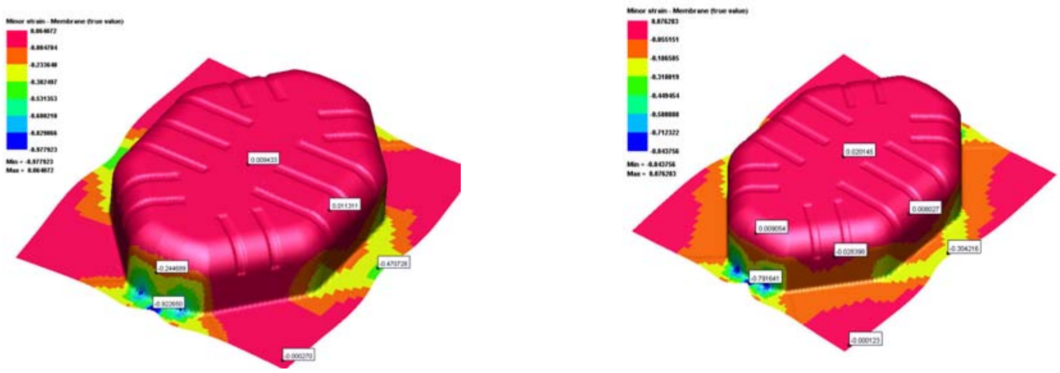

Figure 5.79: Minor strain results with r values of 2.92, 1.1, 2.92 and R value of 2.01.

According to the figures 5.74 - 5.79, results of the simulations change significantly since there is no sign of potential cracking zone in the FLD diagram. Diminishing of r_{45} coefficient is not trigger the strain paths to enter into the cracking zone. Similar results were obtained in previous sections while comparing Lankford coefficients one by one.

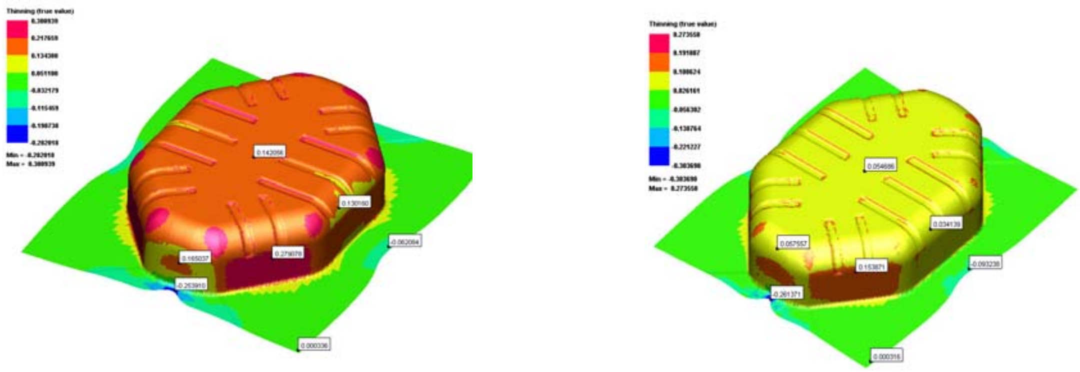

Figure 5.80: Thinning results with r values of 2.5, 2.28, 1 and R value of 2.01

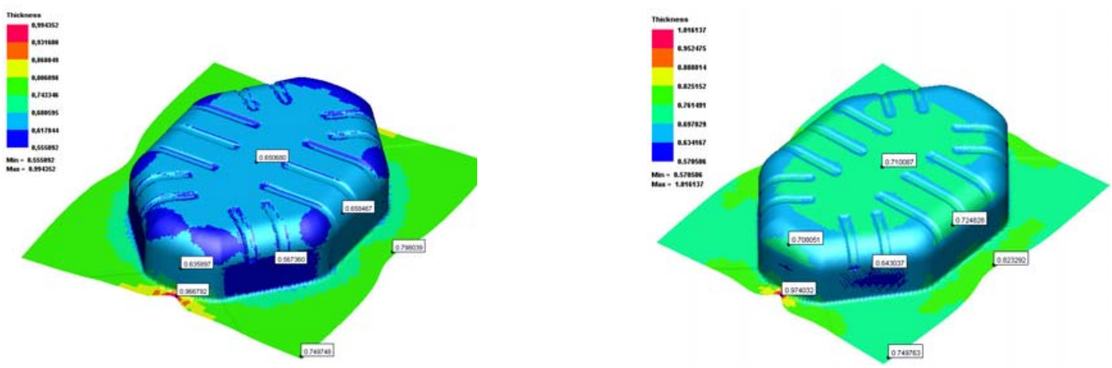

Figure 5.81: Thickness results with r values of 2.5, 2.28, 1 and R value of 2.01

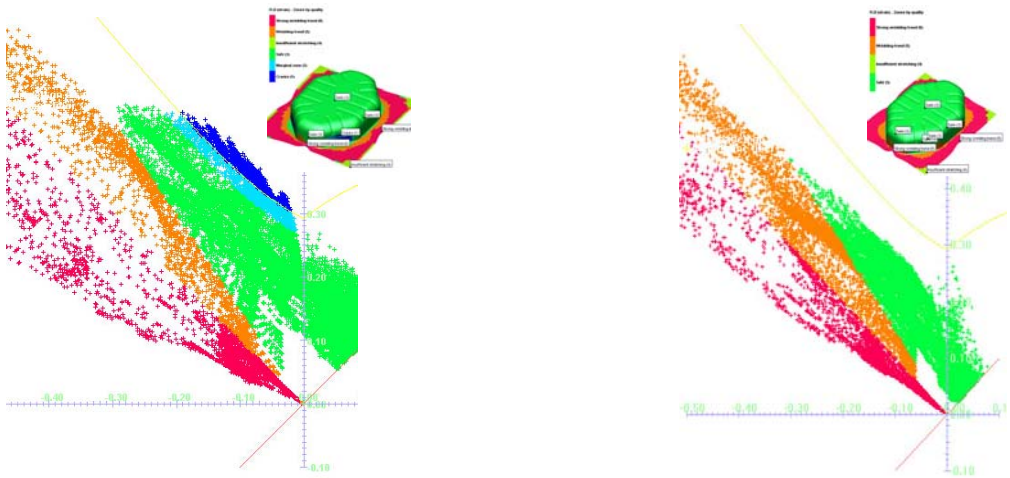

Figure 5.82: FLD results with r values of 2.5, 2.28, 1 and R value of 2.01

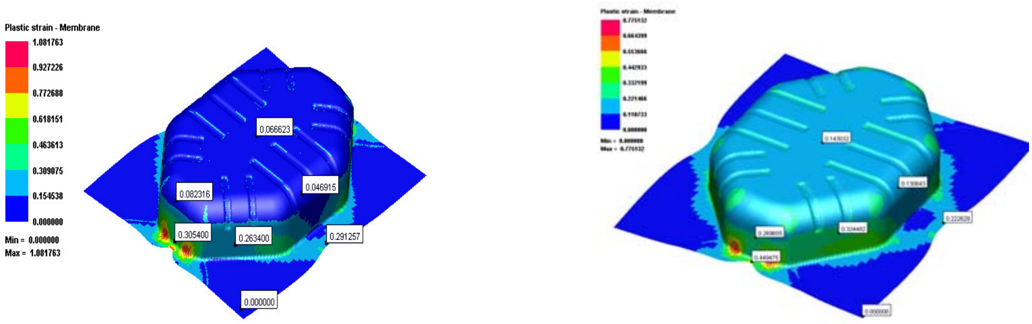

Figure 5.83: Plastic strain results with r values of 2.5, 2.28, 1 and R value of 2.01

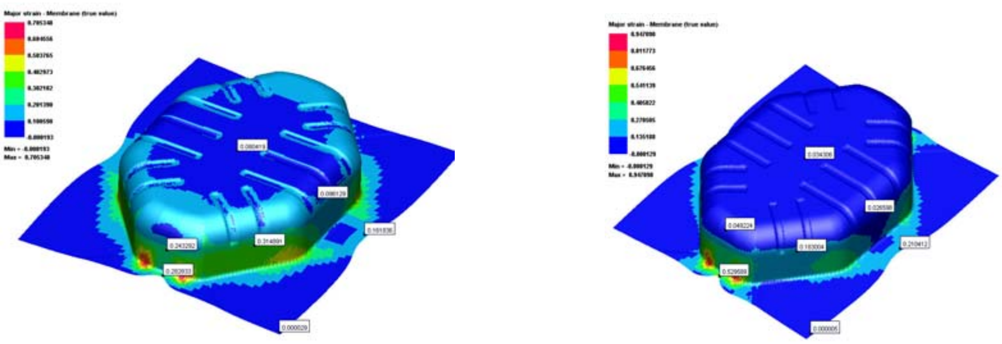

Figure 5.84: Major strain results with r values of 2.5, 2.28, 1 and R value of 2.01

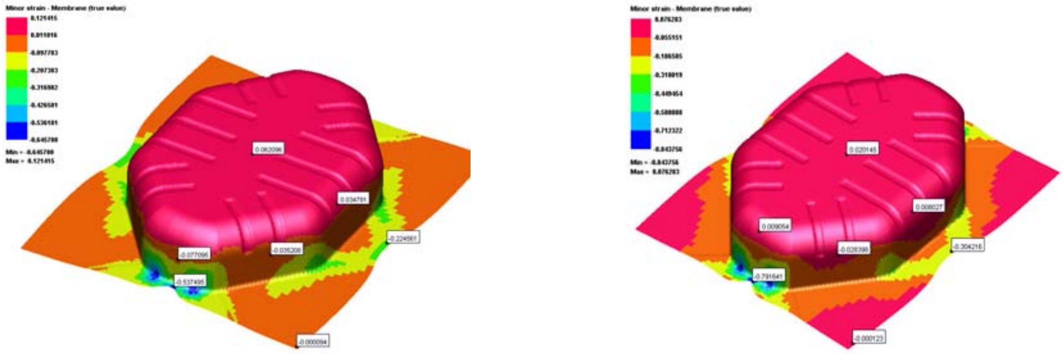

Figure 5.85: Minor strain results with r values of 2.5, 2.28, 1 and R value of 2.01

According to the figures 5.80 - 5.85, results of the simulations vary significantly. Results with the Lankford coefficients are also indicate the sign of a failure. From this point of view, avability of such kind of distribution for Lankford Coefficients must be considered.

6. CONCLUSIONS AND RECOMMENDATIONS

As it is well known, desired final shape of the parts is leaded by the material behaviour. From this view, characterization of material behaviours under several deformation modes such as uniaxial tension, pure shear, uniaxial compression, plane strain etc. is very significant for the development of the process. Before using the materials, related test must be made to figure out the limits of the material.

By using computers, process for desired geometry simulated by calculation of equations which are strain hardening, yielding criteria and hardening type. For this reason, measurements for material characterization and selections for deriving equations are significant for accurate results.

The results of simulations nearly observed in the actual data. Locations of tearing and the regions prone to wrinkling are observed and precautions were made to obtain the desired final shape.

As it is obtained from simulations, results with Lankford Coefficients and normal anisotropy value which is obtained from the same Lankford Coefficients yield different results if value of one of these coefficients is not close to others. On the other hand, availability of such kind of condition might be subjected to another survey.

In this thesis, results for kinematic hardening which is known for its better accuracy could not be obtained, because of the coefficient data for the yielding criteria using kinematic hardening rules was not available. Additionally, results obtained by using kinematic hardening give more accurate results especially for springback problems regarding to the papers related to this field. So, the ways of using this hardening models must be searched for further development.

REFERENCES

[1] **Marciniak, Z., Duncan, J.L., and Hu, S.J.,** 2002. Mechanics of sheet metal forming, Butterworth-Heinemann.

[2] **Arwidson, C.,** 2005. Numerical Simulation of Sheet Metal Forming for High Strength Steels, Licentiate Thesis, Lulea University of Technology, Sweden, ISSN 1402-1757.

[3] **Hu, W., He, J.,** Anisotropic Behaviors and Its Application on Sheet Metal Stamping Proceses, ETA-Engineering Technology Associates, Inc.

[4] **Gau, J.T.,** 1999.A Study of the Influence of the Bauschinger Effect on Springback In Two-Dimensional Sheet Metal Forming, Ph.D. Thesis, School of The Ohio State University, USA.

[5] **Schuler GmbH.,** 1998. Metal Forming Handbook , Göppingen, Germany, ISBN 3-540-61185-1.

[6] **Butuc, M.C.,Gracio, Barata da Rocha, J.J., A.,** 2002. A theoretical Study on Forming Limit Diagrams Prediction, Journal of Material Processing Technology, 714-724

[7] **Hill, R.,** 1950**.** The Mathematical Theory of Plasticity, Oxford University Press, New York,USA.

[8] **Xu, S., Weinmann, K.J.,** 1999. Comparison of Hill's Yield Criteria in Forming Limit Predictions, SAE Technical Paper Series, 1999-01-0999.

[9] **Friedman, P.A., Pan, J.** 1998. Effects of plastic Anisotropy and Yield Criteria on Prediction of Forming Limit Curves, International Journal of Mechanic Sciences 42 (2000) 29-48

[10] **Önder, İ.E.,** 2005. Assesment of Sheet Metal Forming Processes by Numerical Experiments, MSC. Thesis, METU

[11] **Çiçek, O.,** 2005. Effects of Drawbeads in Sheet Metal Forming, MSC. Thesis, ITU

[12] **Hu, W., Liu, S.-D.,** 2002. Enhancement of Yield Criteria Considering Anisotropic Behaviors of Sheet Metals, SAE Technical Paper Series, 2002-01-0158, ISSN 0148-7191

[13] **Johnson, W., Mellor, P.B.,** 1983. Engineering Plasiticity, Ellis Horwood Limited, Chichester, England.

[14] **Altan, T.,** 2004, Short Course on Sheet Metal Forming, Material Properties and Formability, The Ohio State University, Columbus, Ohio.

[15] **Altan, T.,** 2004, Short Course on Sheet Metal Forming, Friction and lubrication in Sheet Metal Forming, The Ohio State University, Columbus, Ohio.

[16] **Altan, T.,** 2004, Short Course on Sheet Metal Forming, Bending, The Ohio State University, Columbus, Ohio.

[17] **Altan, T.,** 2004, Short Course on Sheet Metal Forming, Flanging and Hemming, The Ohio State University, Columbus, Ohio.

[18] **Altan, T.,** 2004, Short Course on Sheet Metal Forming, Deep Drawing of Round Cups, The Ohio State University, Columbus, Ohio.

[19] **Altan, T.,** 2004, Short Course on Sheet Metal Forming, Bending, The Ohio State University, Columbus, Ohio.

[20] **Altan, T.,** 2004, Short Course on Sheet Metal Forming, Introduction to Sheet Metal Forming Process, The Ohio State University, Columbus, Ohio.

[21] **Geng, L., Wagoner, R.H.,** 2002. Role of Plastic Anisotropyt and ıts Evolution on Springback, International Journal of Mechanical Science 44(2002) 123 – 148.

[22] **Sadagopan, S., Urban, D.,** 2003, Formability Characterization of a new generation of high strength steels,AISI/DOE Technology Roadmap Program Final Report, Pittsburg

[23] **Lumin G.,** 2000. Application of Plastic Anisotropy and Non-Isotropic Hadening To Springback Prediction, Ph.D. Thesis, The Ohio State University, Columbus, Ohio.

[24] **Kim, J.-B.,Yang,D.-Y.,Yoon J.-W.,Barlat, F.,** 2000. The Effect of Plastic Anisotropy on Compressive Instability in Sheet Metal Forming, International Journal of Plasticity, 16(2000) 649-676

[25] **Worswick, M.J., Finn, M.J.,** 2000. The Numerical Simulation of Stretch Flange Forming, International Journal of Plasticity, 16(2000) 701-720

[26] **Pam Stamp 2G**, Version 2004.1, 2005. PAMSTAMP-2G User's Guide, Parc Club du Golf 13856 Aix en Provence cedex 3 France.

[27] **Vial-Edwards, C.,** 1997. Yield Loci of FCC and BCC Sheet Metals, International Journal of Plasticity, Vol. 13, No. 5, pp.521-531.

[28] **Green, D.E.,Black, K.C.,** 2002. A Visual Technique to Determine the Forming Limit for Sheet Materials, SAE Technical Paper Series, 2002-01-1062.

[29] **Issa, J.,** 2004. Forming Limit Diagrams, MSc. Thesis, Michigan State University.

[30] **Uk Youn, C.**, 1993. Plane Strain Finite Element Analysis of Sheet Forming operations Including Bending Effects, Ph.D. Thesis, The Ohio State University, Columbus, Ohio.

[31] **Pam Stamp 2G**, Version 2004.1, 2005. PAMSTAMP-2G Reference Manual, Parc Club du Golf 13856 Aix en Provence cedex 3 France.

[32] **Wang, C.,** 1993. Mechanics of Bending, Flanging, and Deep Drawing and a Computer-Aided Modeling System for Predictions of Strain, Fracture, Wrinkling and Springback in Sheet Metal Forming, Ph.D. Thesis, The Ohio State University, Columbus, Ohio.

BIBLIOGRAPHY

Göktuğ ÇINAR was born in Tekirdağ at 1977. He enrolled Mechanical Engineering Department at Istanbul Technical University in 1997. He was graduated from this department in 2002. His master education at Solid Mechanics Program of the Mechanical Engineering Department in ITU is going on and he also works as process and quality engineer at Tool & Die and Prototype Manufacturing Department in Ford-Otosan.